

**Distribution Agreement**

In presenting this thesis as a partial fulfillment of the requirements for a degree from Emory University, I hereby grant to Emory University and its agents the non-exclusive license to archive, make accessible, and display my thesis in whole or in part in all forms of media, now or hereafter now, including display on the World Wide Web. I understand that I may select some access restrictions as part of the online submission of this thesis. I retain all ownership rights to the copyright of the thesis. I also retain the right to use in future works (such as articles or books) all or part of this thesis.

Riley Brackin

April 8, 2023

The Influence of Polymer Molecular Weight on Hyaluronic Acid Hydrogel Reinforcement of  
Articular Cartilage

by

Riley Brackin

Dr. Jay Patel  
Adviser

Chemistry

Dr. Jay Patel  
Adviser

Dr. Craig Hill  
Committee Member

Dr. Ben Miller  
Committee Member

2023

The Influence of Polymer Molecular Weight on Hyaluronic Acid Hydrogel Reinforcement of Articular Cartilage

By

Riley Brackin

Dr. Jay Patel  
Adviser

An abstract of  
a thesis submitted to the Faculty of Emory College of Arts and Sciences  
of Emory University in partial fulfillment  
of the requirements of the degree of  
Bachelor of Science with Honors

Chemistry

2023

## Abstract

# The Influence of Polymer Molecular Weight on Hyaluronic Acid Hydrogel Reinforcement of Articular Cartilage

By Riley Brackin

**Introduction:** Osteoarthritis (OA) is a degenerative joint disease that often results from traumatic injury and causes significant disability. The disease is typically characterized by a gradual breakdown of articular cartilage, which is normally a dense extracellular matrix (ECM). As the degradation progresses, the ECM breaks apart, triggering a cascade of inflammatory signaling, including tumor necrosis factor- $\alpha$  (TNF- $\alpha$ ) and interleukin-1-beta (IL-1 $\beta$ ), which prompt the production of matrix-degrading enzymes. This perpetuates a cycle of further joint breakdown, ultimately contributing to the pathogenesis of osteoarthritis. Recent studies demonstrated that cartilage-infiltrating biomaterials can reinforce damaged cartilage and slow down the degradation of the ECM. This study specifically focuses on how the molecular weight of methacrylated hyaluronic acid (MeHA) impacts biomechanical fortification and preservation of articular cartilage in a pro-degradation environment.

**Materials and Methods:** MeHA (20 kDa, 75 kDa, and 100kDa) was synthesized and the degree of methacrylation of each was confirmed with NMR. The three hydrogel polymers were applied to juvenile bovine cartilage explants. Hydrogel mechanical testing was performed, and initial diffusion studies were conducted to confirm hydrogel infiltration into cartilage. Fortified cartilage explants were cultured for a two-week degradation period (10ng/mL IL-1 $\beta$ ), during which media was sampled for proteoglycan loss. Explants were mechanically tested via Hertzian Indentation creep tests at the end of this two-week period.

**Results:** The degree of methacrylation was 30.28%, 35.5%, and 55.9% for the 20 kDa, 75 kDa, and 100 kDa polymers, respectively. All polymers produced significantly different compressive modulus values ( $p$ -value $<0.0001$ ). The 20 kDa MeHA applied to articular cartilage explants showed a significantly higher compressive modulus with the control condition,  $p$ -value $<0.001$ , and IL-1 $\beta$  condition,  $p$ -value $<0.01$ .

**Discussion:** The cartilage explants showed promising reinforcement with the 20 kDa MeHA polymer condition, particularly regarding compressive modulus. This suggests that a greater diffusion ability and distance are likely beneficial for mechanical reinforcement of cartilage, resulting in maintenance of these biophysical properties in degenerative conditions.

**Clinical Relevance:** Using MeHA with a smaller molecular weight may be beneficial in maintaining mechanical properties and proactively reducing articular cartilage degeneration.

The Influence of Polymer Molecular Weight on Hyaluronic Acid Hydrogel Reinforcement of Articular Cartilage

By

Riley Brackin

Dr. Jay Patel  
Adviser

A thesis submitted to the Faculty of Emory College of Arts and Sciences  
of Emory University in partial fulfillment  
of the requirements of the degree of  
Bachelor of Science with Honors

Chemistry

2023

## Acknowledgements

I express my sincere gratitude to my research advisor, Dr. Jay Patel, for this remarkable opportunity. My experience in the Patel Lab has been invaluable, and I am profoundly appreciative of all the knowledge I have acquired under his guidance. Dr. Patel's constant support and mentorship have significantly contributed to my future pursuits.

Furthermore, I extend my appreciation to Gail McColgan for her unwavering patience, Dr. Ben Miller for his valuable guidance on the best practices of academic writing, and Dr. Craig Hill for his exceptional teaching methods that made learning chemistry such an enjoyable experience.

## Table of Contents

1. Introduction.....	2
1.1 Knee Joint Anatomy and Physiology .....	2
1.2 Motivation.....	4
1.3 Osteoarthritis .....	5
1.4 Hydrogels to Combat Chondrocyte Degeneration .....	10
1.5 Objectives and Significance.....	12
2. Materials and Methods.....	14
<i>Aim1: Methacrylation of Hyaluronic Acid and Gel Mechanics .....</i>	<i>14</i>
2.1 Methacrylate Hyaluronic Acid Reaction.....	14
2.2 Gel Mechanics .....	17
<i>Aim 2: MeHA Hydrogel Diffusion .....</i>	<i>17</i>
2.3 Explant Dissection and Processing .....	17
2.4 Diffusion Studies (integration and fortification) .....	18
<i>Aim 3: Application of MeHA to Living Explants .....</i>	<i>19</i>
2.5 Living Explant Degenerative Culture .....	19
2.6 Mechanical Testing of Degenerative Culture.....	21
2.7 DMMB Assay.....	23
2.8 Safranin-O Fast Green Staining.....	23
2.9 Statistical analysis.....	24
3. Results .....	25
<i>Aim 1: Methacrylation of Hyaluronic Acid and Gel Mechanics .....</i>	<i>25</i>
3.1 NMR of MeHA Polymers with Interpretations .....	25
3.2 Gel Mechanics.....	28
<i>Aim 2: MeHA Hydrogel Diffusion .....</i>	<i>30</i>
3.3 Tissue Penetration of Degenerated Cartilage Images of Diffusion.....	30
<i>Aim 3: Application of MeHA to Living Explants .....</i>	<i>31</i>
3.4 Living Cartilage Explant Mechanics .....	31
3.5 Proteoglycan Loss .....	33
3.6 Imaging .....	35
4. Discussion.....	37
5. Conclusion .....	43
6. Supplementary Information.....	44
7. References.....	46

## 1. Introduction

### 1.1 Knee Joint Anatomy and Physiology

The largest hinge joint in the body is the knee joint. It consists of three bones: the femur, tibia, and patella (Figure 1). The femur is the upper leg bone and connects to the lower leg bones, the tibia, and fibula, at the knee joint.<sup>1</sup> The bones are held together by a joint capsule consisting of two distinct layers. The outer layer of dense connective tissue and an inner membrane called the synovium secretes a fluid to lubricate the joint. The synovium mediates nutrient exchange between blood and joint fluid as cartilage lacks blood vessels.<sup>1,2</sup> A layer of articular cartilage covers the entire articulating surface of the tibia and femur, providing load distribution, shock absorption, and lubricated smooth motion. These features are certainly present in the knee, but also in joints across the entire body.

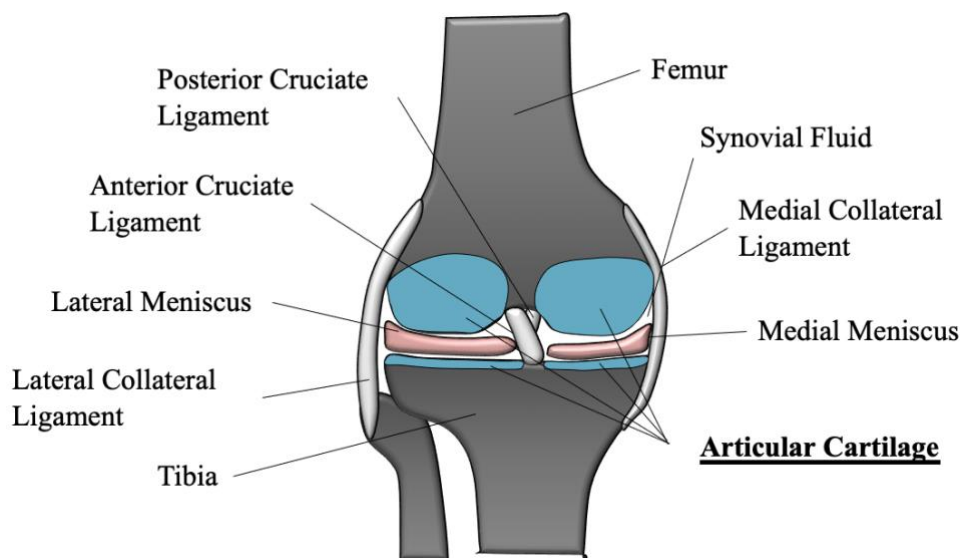


**Figure 1.** The knee joint is complex and made up of several components, including bones, ligaments, cartilage, and muscles. The knee joint connects the femur (thigh bone), the tibia (shin bone), and the patella (kneecap). These bones are held together by ligaments and surrounded by muscles. There are two types of cartilage in the knee joint: articular cartilage and meniscus cartilage. Articular cartilage covers the ends of the femur and tibia bones, while the meniscus cartilage is located between the femur and tibia bones. The cartilage within the knee help to cushion the joint and prevent bones from rubbing against each other. The knee joint also contains synovial fluid, which lubricates the joint and helps to reduce friction between the bones.

Articular cartilage is a viscoelastic material exhibiting both viscous and elastic characteristics. As a highly specialized connective tissue of diarthrodial joints, articular cartilage provides a smooth, lubricated surface for articulation and facilitates the transmission of loads with a low frictional coefficient.<sup>3</sup> Articular cartilage consists of a sparsely distributed and highly specialized cells called chondrocytes embedded within a dense extracellular matrix ECM.<sup>4</sup> The ECM is principally composed of water, collagen, and proteoglycans. These components carry a negative charge are crucial for water retention and maintaining the mechanical properties of cartilage.<sup>3</sup> Zonal variations in structure and composition within the collagen fiber and ECM exist. The zones are the superficial zone, the middle zone, the deep zone, and the calcified zone (Figure 2). The integrity of the superficial zone is imperative in protecting and maintaining deeper layers. The superficial zone makes up 10% to 20% of the hyaline cartilage thickness and contains a relatively high number of flattened chondrocytes. Chondrocytes at this level are flatter, smaller, and generally have a greater density than the cells deeper in the matrix. Each chondrocyte establishes a specialized microenvironment and is responsible for the turnover of the ECM in its immediate vicinity. Chondrocytes contain gap-junctions for direct cell-to-cell communication and signal transduction.<sup>3</sup> Additionally, they respond to a variety of signaling molecules including cytokines, growth factors, and extracellular matrix molecules, as well as, mechanical loads, piezoelectric forces, and hydrostatic pressures.<sup>5</sup>

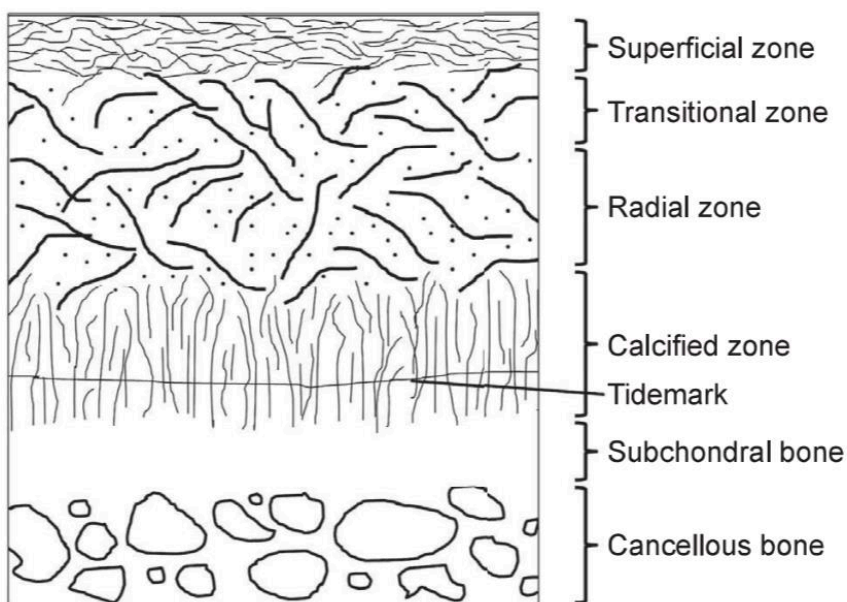


**Figure 2.** Articular cartilage is a smooth tissue that covers the ends of bones in joints. It has four layers: a superficial layer, a middle layer, a deep layer, and a calcified layer. The superficial layer provides stability and smooth motion, the middle layer distributes weight, the deep layer absorbs shock, and the calcified layer anchors the cartilage to the underlying bone. These layers work together to cushion the joint, provide stability, and ensure proper function.<sup>3</sup>

## 1.2 Motivation

Osteoarthritis (OA) is the most common form of joint disease.<sup>6</sup> OA has a prevalence of 58.5 million US adults in the general population. Over half (57.3%) of this population are 18 to 64 years old in the working class.<sup>7</sup> In addition to the physical effects of OA (pain, discomfort, reduced quality of life), it carries a significant economic burden. OA is the leading cause of work disability and contributes an estimated \$303.5 billion in combined medical care cost and loss, annually.<sup>7,8</sup> OA is even more prevalent in the military and Veteran population (Figure 3). Over one in three Veterans have arthritis, 35%, compared to about one in four civilians, 23.7%, that have arthritis.<sup>9</sup> Even with this enormous market, there are limited curative therapies.

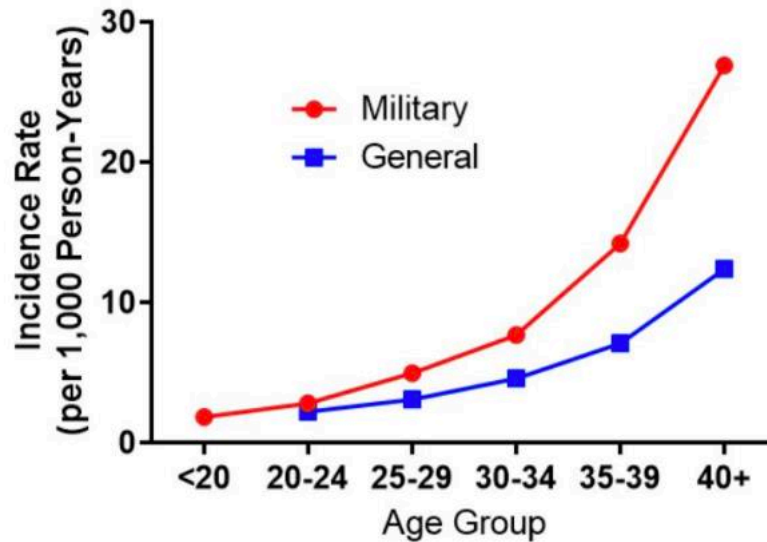


**Figure 3.** The incidence rate of osteoarthritis per age group in the veteran population, red, compared to the civilian population, blue, is depicted above. (Data from Cameron et al<sup>10</sup>)

### 1.3 Osteoarthritis

OA is a chronic condition most common in the knee joint. The most common risk factors for OA include obesity, joint injury, surgery, aging, and a family history of arthritis.<sup>6</sup> The deteriorative effects cause joint pain, particularly during movement or weight-bearing activities, stiffness, especially after prolonged periods of inactivity, swelling or tenderness around the knee joint, limited range of motion, and bone spurs forming around the knee joint. OA is characterized by breakdown of the entire joint, including bone, cartilage, ligaments, and the synovium.<sup>11</sup> The extent of the harm often remains unrealized until the patient experiences pain, often after a significant amount of the articular cartilage deteriorates. The degenerative disease is propagated through biochemically mediated interactions causing the breakdown of articular cartilage extracellular matrix (ECM) and synovial inflammation, leading to alterations in the knee environment and function.<sup>12,13</sup>

The patient's presentation is rooted in the previously homeostatic joint environment. Stress initiation of several inflammatory pathways triggers impairment of joint homeostasis. More substantial matrix degradation replaces a healthy cartilage turnover, resulting in net

cartilage tissue loss.<sup>12</sup> Specifically, the development of OA involves two important pro-inflammatory cytokines, namely interleukin-1-beta (IL-1 $\beta$ ) and tumor necrosis factor-alpha (TNF- $\alpha$ ). These cytokines act as signaling molecules to increase cartilage breakdown by stimulating matrix metalloproteinase (MMPs) activity.<sup>14</sup> These activated MMPs target specific ECM proteins, mainly type II collagen, and aggrecan, leading to their degradation.<sup>12</sup> As the ECM breaks apart, small pieces of it can attach to the membranes of synoviocytes. These attachments trigger a chain reaction of inflammatory responses that produce pro-inflammatory cytokines like tumor necrosis factor-alpha (TNF- $\alpha$ ) and interleukin-1-beta (IL-1 $\beta$ ). These cytokines can then bind to chondrocytes and prompt them to produce even more MMPs, specifically MMP-13 and MMP-3.<sup>14</sup> The increased production of these MMPs accelerates the breakdown of cartilage, which perpetuates a vicious cycle of synovial inflammation and further ECM breakdown, ultimately contributing to the pathogenesis of osteoarthritis.

Inflammatory imbalances influence the remodeling and growth of the subchondral bone, the layer of bone just beneath the articular cartilage, through interactions between the bone and cartilage<sup>11,15</sup> (Figure 4). The critical role of inflammation is observed in osteoblasts, bone building osteocytes, which express pro-inflammatory phenotypes during the breakdown of articular cartilage<sup>16</sup>. This increased cytokine signaling promotes subchondral bone sclerosis, or thickening of the bone, and contributes to the further degradation of the cartilage extracellular matrix by activating chondrocyte production of MMP-13 and MMP-3<sup>17</sup>. Additionally, when joints experience mechanical overload, bone marrow lesions are the initial signs of degeneration and likely signify a reparative response. Following bone marrow lesions, subchondral bone remodeling increases bone volume but reduces bone mineral density.

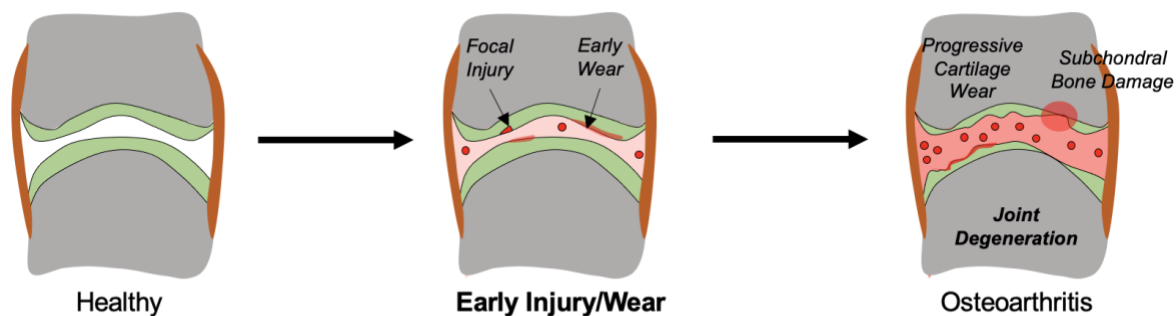


**Figure 4.** Inflammatory imbalances, such as those seen in osteoarthritis, can influence the remodeling of the subchondral bone, the layer of bone just beneath the articular cartilage in joints. In osteoarthritis, there is an imbalance between the breakdown and synthesis of the extracellular matrix in the subchondral bone. This leads to increased bone resorption, or breakdown, and decreased bone formation. As a result, there is a decrease in bone density and distortions in the subchondral bone structure. The resulting changes in subchondral bone structure contribute to joint pain and stiffness.

A phenotype that often arises in OA patients are bone and cartilage growths at the edges of the articular cartilage. The growth is referred to as osteophytes, also known as bone spurs or bony lumps. Mesenchymal cells (MSC) create osteophytes in the periosteum, which is the tissue that covers the outer surface of bones. It is hypothesized that inflammatory signals from the synovial cavity trigger the proliferation of these MSCs.<sup>18</sup> Osteophytes are a repair mechanism to stabilize the knee joint following cartilage damage.<sup>19</sup> However, the presence of osteophytes is often associated with pain and loss of joint mobility, which can further worsen the condition of OA.

Overall, the interactions between the synovial membrane and the immune system play a crucial role in the development and progression of OA. The breakdown of articular cartilage releases ECM proteins, which are then phagocytosed by macrophage-like synoviocytes (MLS) and activate the NF- $\kappa$ B pathway. This pathway produces and releases pro-inflammatory cytokines, such as TNF- $\alpha$  and IL-1 $\beta$ , into the synovial fluid, creating a pro-inflammatory environment within the joint. This chronic inflammation further attracts immune cells to the

joint, which promotes a destructive cycle of inflammation, cartilage loss, subchondral bone remodeling, and osteophyte formation (Figure 5). Therefore, understanding the mechanisms of synovial inflammation and cytokine signaling is critical in developing targeted therapies for OA.

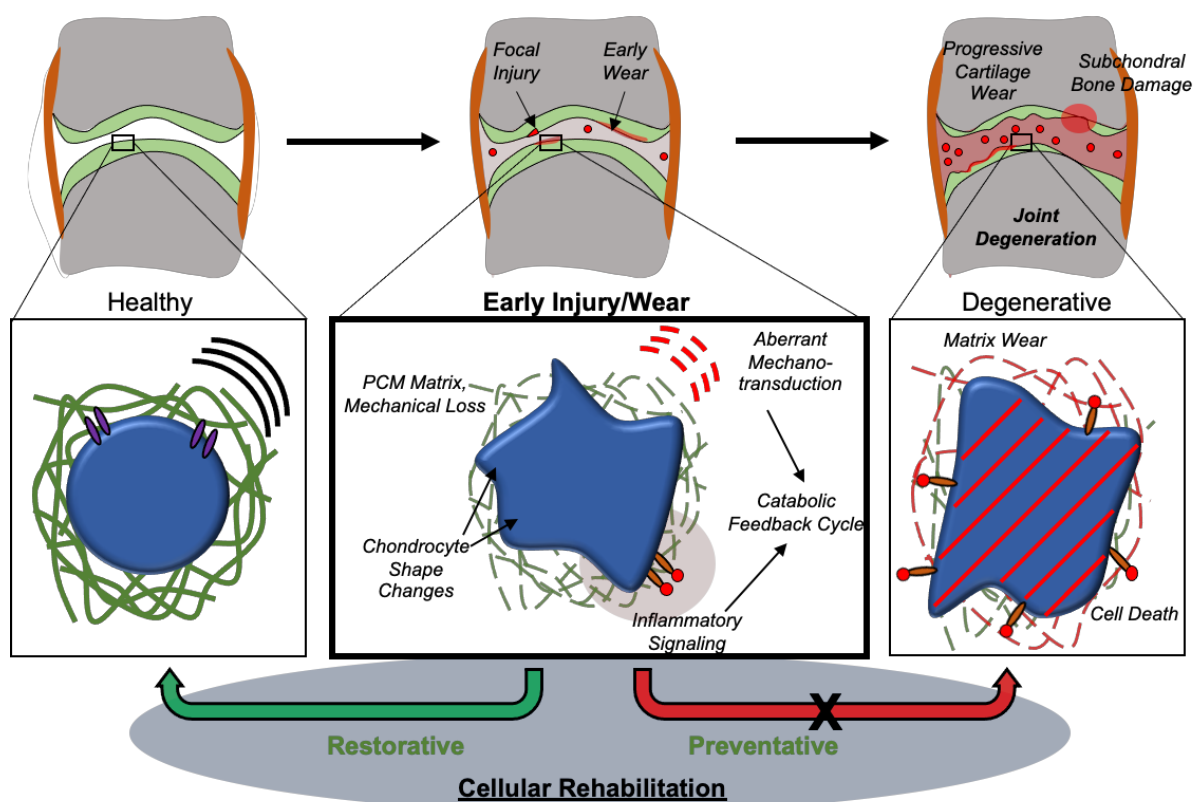


**Figure 5.** As the joint degrades, it can go one of two ways, restoration or perpetuation down the vicious cycle of degeneration. Fortification of the articular cartilage can decrease the degenerative process and lead to restoration. On the contrary, cytokine signaling balance can shift further towards inflammation and cartilage destruction. This leads to a vicious cycle of joint degradation and inflammation, ultimately resulting in pain, stiffness, and loss of function associated with osteoarthritis.

Studies have identified several cytokines contributing to OA pathogenesis, including  $\text{TNF-}\alpha$ ,  $\text{IL-1}\beta$ ,  $\text{IL-6}$ ,  $\text{IL-17}$ , and  $\text{IL-18}$ .<sup>20</sup> Targeting these cytokines with biological agents, such as monoclonal antibodies, drugs, or injections have shown promise in reducing inflammation and improving symptoms in OA patients (Figure 6). However, these are short term solutions as biologics are quickly cleared from the joint. Cartilage-infiltrating hydrogel could be the solution

to long term relief due to the longevity of the hydrogel cartilage interaction. Overall, a better understanding of synovial inflammation and immune cell interactions in OA can lead to the development of more effective treatments for this debilitating condition.

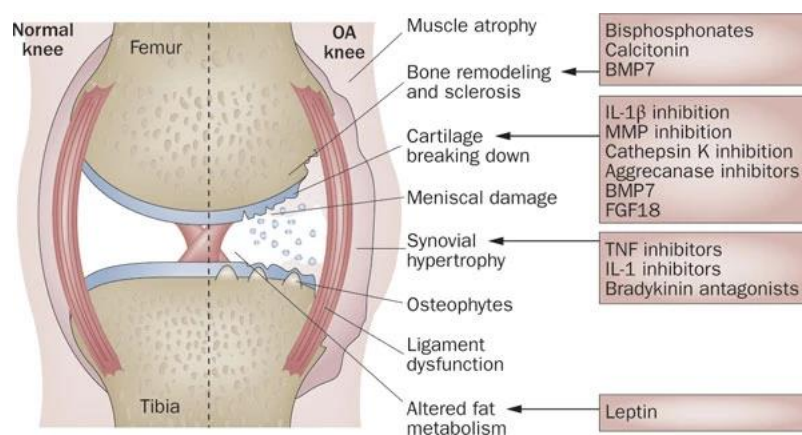


**Figure 6.** Illustration of agents that target relevant tissues in knee of an OA patient. OA is a complex disease with various pathogenic factors involved in its progression, including inflammation, cartilage degeneration, subchondral bone remodeling, and synovial tissue alterations. Therefore, multiple targets for OA have been identified to help develop effective treatments for this disease.<sup>14</sup>

The damage will continue to decline as long as the joint environment permits. The avascularity of the tissue limits the intrinsic healing capacity, boosting the need for proactive intervention. Clinically, the most effective means of diagnosing OA is through histological analysis of biopsy obtained samples.<sup>21</sup>

The current gold standard in surgical therapies for damaged cartilage involves the removal of damaged tissue, repair via direct fixation, marrow stimulation, and transplantation utilizing autograft or allograft tissue.<sup>22</sup> While these interventions have provided short-term symptomatic relief, they have fallen short in delivering long-term comfort due to the mechanically inferior quality of the generated cartilage and the difficulty in integrating transplanted tissue with existing cartilage.<sup>23</sup>

Recent research in tissue engineering and regenerative medicine has shown promise in developing new cartilage repair and regeneration approaches. These approaches aim to create functional hyaline cartilage that can integrate seamlessly with existing cartilage and provide long-term mechanical stability. However, these therapies, while promising, have not shown consistent efficacy preclinically or clinically, and thus methods to preserve cartilage are still of great interest.

The complexity of producing mechanically durable hyaline cartilage puts importance on preservation and proactive therapies to reduce progressive degeneration. Recent studies have found success in utilizing biomaterials to “stabilize” existing cartilage, focusing on the biomechanical fortification of the tissue.<sup>24,25</sup> Both natural and synthetic hydrogels show the potential to resurface or interpenetrate damaged cartilage, improving biphasic mechanical properties of degenerated cartilage.<sup>26</sup> However, a gap remains in evaluating the response of chondrocytes following this initial application, especially in inflammatory conditions that are often present post-injury.

#### 1.4 Hydrogels to Combat Chondrocyte Degeneration

Previously, a similar hyaluronic acid (HA) hydrogel biomaterial diffused into defective cartilage, improved the initial mechanics of degenerated cartilage, and remained for at least seven days *in vivo*<sup>24</sup>. Another study confirmed HA-based hydrogel interpenetration with cartilage tissue to reinforce surface-damaged cartilage and prevent catabolic deterioration.<sup>27</sup> This study was focused on gel application after structural degeneration occurred. Therefore, the study specifically investigated hydrogel application on focal defects below the superficial layer. In a degenerative culture model, HA application mitigated biomechanical and biochemical loss and

reduced chondrocyte catabolic response. These results present evidence of both time-zero and prolonged benefits from an HA-based cartilage stabilization strategy to delay the progression of cartilage deterioration. In this thesis, we reproduce a degenerative culture model to focus on establishing characteristics surrounding the HA cartilage-fortifying method at the superficial zone. We seek to identify if superficial application provides not only initial reinforcement but also prolonged preservation of the biomechanical and biochemical health of cartilage, with an emphasis on determining the impact of HA molecular weight.

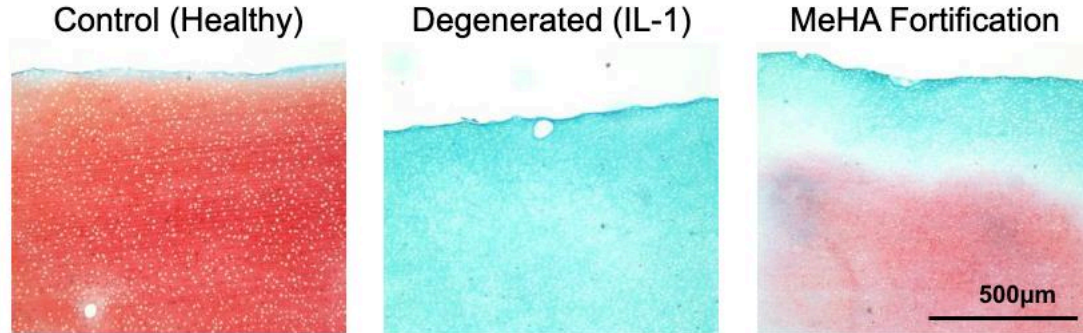


**Figure 7.** Methacrylated hyaluronic acid (MeHA) is a modified form of hyaluronic acid cross-linked to form a hydrogel. MeHA hydrogels have high water content and can provide lubrication to the joint, reduce friction, and have anti-inflammatory properties. MeHA hydrogels have potential applications in the treatment of osteoarthritis, including as a drug delivery vehicle for anti-inflammatory agents and as a biomaterial for cartilage fortification and regeneration.<sup>27</sup>

## 1.5 Objectives and Significance

The goal of this thesis is to utilize a degenerative culture model to establish the protection of the HA cartilage-fortifying method, specifically at the superficial level. Additionally, to characterize the relative impact on diffusion, integration, fortification, and protection, I varied the molecular weight of the HA hydrogel precursor. Theoretically, the smaller molecular weight polymer will have a greater diffusion into the cartilage. However, the smaller MW polymer exhibits a lower stiffness than the larger molecular weight polymers, likely creating a relatively less stiff cartilage-penetrating gel compared to the other MW polymers. The interplay of diffusion and mechanical reinforcement of cartilage will better characterize the method of HA reinforcement.

To achieve this goal, I investigated three specific aims. The first aim was to methacrylate HA polymers and perform hydrogel mechanical testing (Figure 7). My second aim was to characterize the relative diffusions of the MeHA gel polymers in nonsterile cartilage explants. Lastly, my third aim was to investigate the protective ability of MeHA applied on live cartilage explants in a two-week sterile degenerative culture. I hypothesized that the smaller molecular weight MeHA polymer would diffuse further and be the most advantageous to maintaining mechanically stable cartilage.

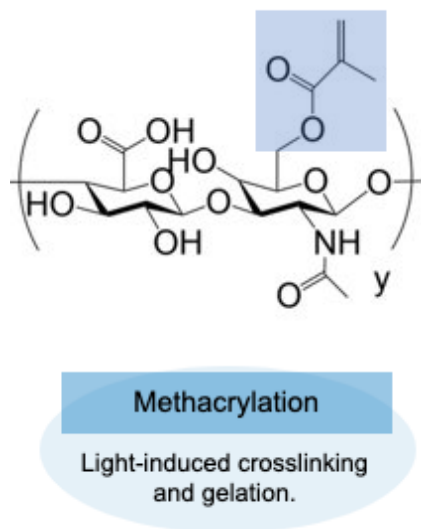


**Figure 8.** Methacrylated hyaluronic acid (MeHA) is a modified form of hyaluronic acid (HA), a natural polysaccharide found in the extracellular matrix of many tissues, including articular cartilage. MeHA is created by adding methacrylate groups to the HA molecule, allowing it to crosslink with other molecules within the joint under specific conditions, forming a hydrogel. This hydrogel integrates in to the articular cartilage and fortifies the mechanical properties of the cartilage, thus increasing its longevity within the joint.<sup>27</sup>

## 2. Materials and Methods

### Aim1: Methacrylation of Hyaluronic Acid and Gel Mechanics

#### 2.1 Methacrylate Hyaluronic Acid Reaction

To methacrylate hyaluronic acid, a coupling reaction proceeds through methacrylate esterification with the hydroxyl group of hyaluronic acid (Fig 8).

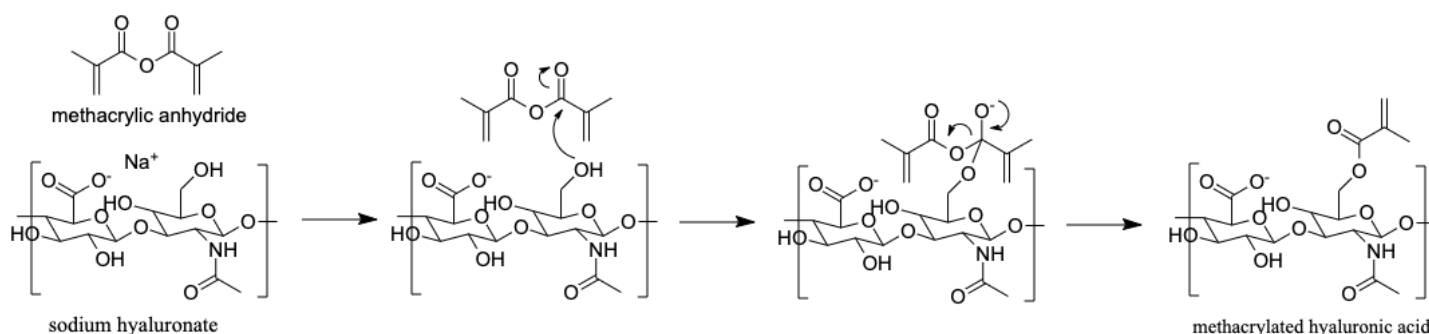


**Figure 9.** Mechanism of hyaluronic acid and methacrylic anhydride to produce methacrylated hyaluronic acid. (Imaged created in ChemDraw).

MeHA was synthesized from sodium hyaluronate (20kDa and 75kDa) and methacrylic anhydride. Sodium hyaluronate was dissolved in deionized water (10 mg/mL, 1% w/v), to which a 20-fold excess of methacrylic anhydride was added. The reaction was maintained at a pH of 8.0-9.0 for 6 hours at 4°C. At the end of the reaction, the solution was stirred vigorously overnight at room temperature to degrade the methacrylic anhydride. The solution was dialyzed (MWCO: 6,500) for 5 days, followed by freezing at -20°C for 6 hours and lyophilization (-50°C, 0.05mbar) for 5 days to produce dry MeHA. 100kDa MeHA was purchased from Advanced Biomatrix (PhotoHA). Nuclear magnetic resonance Spectroscopy (NMR) confirmed the methacrylation of HA on the 20 kDa (MeHA; Advanced biomatrix) polymer, 75 kDa (MeHA; Advanced biomatrix), and the 100 kDa (PhotoHA; Advanced biomatrix) polymer.

Proton Nuclear Magnetic Resonance ( $H^1$  NMR) spectroscopy is an analytical technique derived from a physical phenomenon that occurs when atomic nuclei with an odd number of protons or neutrons, usually  $C^{13}$  or  $H^1$ , are placed in a strong magnetic field and exposed to electromagnetic radiation. Analytical experiments often use this phenomenon to determine molecules' structure, composition, and dynamics. We utilized  $H^1$  NMR to determine the percent methacrylation of our MeHA polymers at 20 kDa, 75 kDa, and 100 kDa. MeHA polymer (~10mg) was dissolved in deuterium oxide ( $D_2O$ ) in thin-walled NMR tubes and imaged at the Emory NMR Core. The NMR spectra was processed using Mnova software. In the Mnova analysis, the solvent peak of deuterium oxide ( $D_2O$ ) was set to 4.79 ppm. Integration was performed on the two protons of the methylene carbon on the methacrylate group at  $\delta$  6.2 ppm and  $\delta$  5.8 ppm in relation to the ten protons of the backbone structure between  $\delta$  3.0–4.2 ppm (Figure 9). The proton peak at  $\delta$  6.2 ppm was set to 1.00 and used to normalize the spectrum. We averaged the integration of the two peaks at  $\delta$  6.2 ppm and  $\delta$  5.8 ppm and divided that value by the integration of  $\delta$  3.0–4.2 ppm and multiplied by 10 protons to obtain the polymer percent methacrylation.<sup>28</sup>

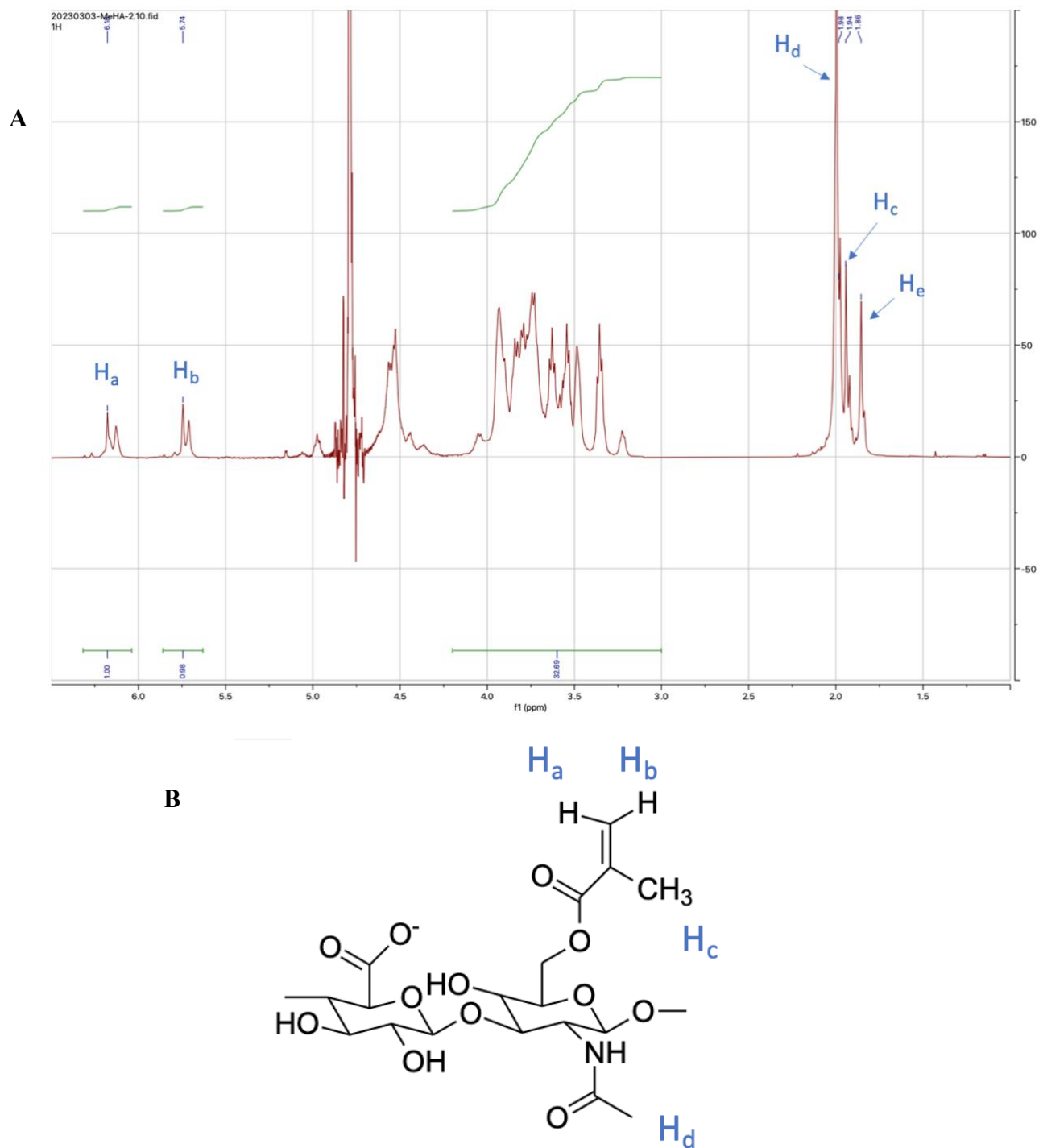


**Figure 10.** The NMR (A) and corresponding molecular structure (B) of the MeHA polymer is depicted above.  $H_a$ ,  $H_b$ , and  $H_c$  peaks correspond to the methacrylated HA hydrogens and were used to determine the percent methacrylation of each MW polymer.  $H_d$  corresponds to the methyl group proton on the N-acetylglucosamine of the HA backbone. The  $H_e$  peak on the NMR corresponds to the remaining unreacted methacrylic anhydride.

## 2.2 Gel Mechanics

Hydrogels alone were formed using 2%, 4%, and 6% formulations of each of the molecular weights, with 0.05% LAP. Cylindrical molds (6mm diameter x 1mm thickness) were used to fabricate gels, which were cross linked for 10 minutes with blue light. Gel mechanics were characterized using an Optics 11 nano-indentation system. A 10-micron radius probe was used to indent gels until an indentation of one micron. Resulting load-deformation curves were fit with a Hertzian Biphasic indentation equation to obtain an effective Young's modulus. Three gels of each MW-% combination were tested, with number indentations per gel.

### Aim 2: MeHA Hydrogel Diffusion

## 2.3 Explant Dissection and Processing

Application of MeHA was performed with cartilage explants from the trochlear groove of juvenile bovine knees. Cartilage explants were taken from the trochlear groove with a 6mm diameter disposable biopsy punch. Cartilage within this site differentiates medially and laterally regarding elasticity and other mechanical properties. I acknowledge these differences and randomize the control and experimental groups with respect to the locations to which these explants are extracted within the groove. In this evaluation, we also have data from multiple donors. After harvest, the calcified cartilage region was removed, to ensure a perpendicular surface. This left top 3mm-6mm of cartilage tissue.

## 2.4 Diffusion Studies (integration and fortification)

Initial diffusion studies were performed to verify interpenetration and retention of the hydrogel in cartilage explants. Three different hydrogel solutions at 20kDa, 75kDa, or 100kDa MeHA (4% w/v, unless otherwise noted) were made. The MeHA polymer was first dissolved in PBS (80% of total volume) using alternating vortexing and centrifugation. Next, light sensitive materials were then added: 10% v/v methacrylated rhodamine (final: 0.025% w/v) and 10% v/v 2,4,6-trimethylbenzoylphosphinate (LAP) (final: 0.05% w/v). Methacrylated rhodamine was added to the MeHA solution for visualization of hydrogel interdigitation as it allows for visualization of the HA polymer material within the cartilage explant. LAP photo-initiator is a water soluble free radical photoinitiator that converts light energy into chemical energy in the form of reactive intermediates, such as free radicals and reactive cations, which subsequently initiate polymerization. We utilize LAP to initiate free radical chain polymerization of the MeHA hydrogel upon light exposure. LAP is photocrosslinked with 405nm blue light. The hydrogel solution is then applied to the articular cartilage explant surface (superficial zone), allowed to diffuse into the cartilage for five minutes, and crosslinked with blue light (400-500nm) for 10 minutes. The explants are then sliced in half vertically, embedded in Optimal cutting temperature compound (OCT), often used to embed tissue samples prior to frozen sectioning, and frozen. The explants were sectioned using a cryostat set to a 20 $\mu$ m section thickness. Sections were rinsed to remove OCT, mounted with ProLong Gold with DAPI, and coverslipped. We utilized a TRITC (Tetramethylrhodamine isothiocyanate) filter to visualize the polymer and a DAPI (4',6-diamidino-2-phenylindole) filter visualize the nucleus. The DAPI filter is designed to transmit light in the ultraviolet range (around 360-390 nm) to collect the blue fluorescence emitted by the

dye (around 410-460 nm).

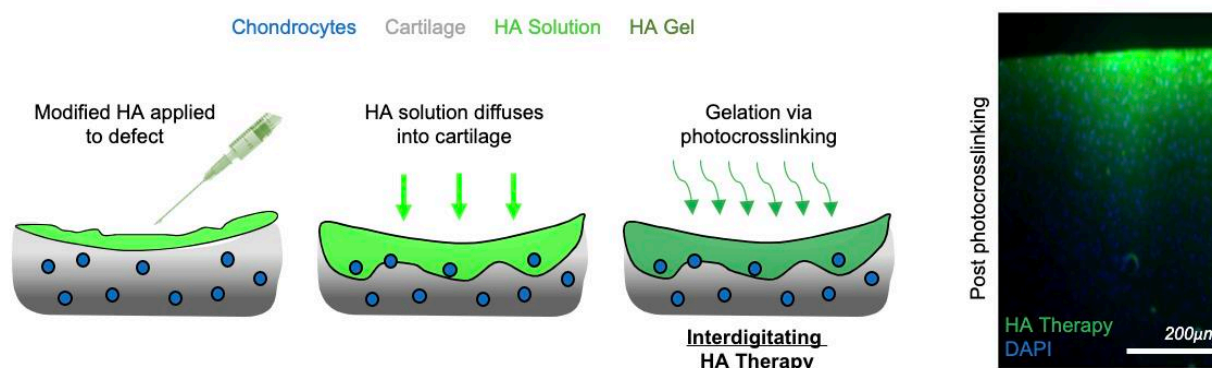


**Figure 11.** The MeHA is applied to the superficial zone of the cartilage explant, allowed to diffuse, and is finally crosslinked. HA is often used as a scaffold material to support the growth of chondrocytes and fortification of the tissue. The interpenetration of HA into cartilage explants can support the mechanical properties of the tissue, such as stiffness and viscoelasticity, which in turn can affect the response of chondrocytes to mechanical loading as well as a reduction in inflammatory cytokines.<sup>27</sup>

### Aim 3: Application of MeHA to Living Explants

#### 2.5 Living Explant Degenerative Culture

Once we extract the cartilage plugs, we culture the explants for two days as an *in vitro* normalization period. After this period, we applied the HA polymer precursor (4% w/v HA with 0.05% w/v LAP), allowed 5 minutes polymer diffusion, and crosslinked under blue light for 10 minutes. We then embed the plugs in agarose wells to confine cartilage samples, exposing only the polymer-coated surface of the cartilage plug to emphasize media exposure to the surface of explants (Figure 12). In creating the agarose wells, we added 1 mL of sterile, liquid agarose (1% w/v) to each well of a 24-well non-treated tissue culture plate and allowed cooling until gel formation. A 6mm disposable biopsy punch was then used to excise agarose to create a well matched to the size of explants. Explants were then treated with either chemically defined media (CM-; Dulbecco's Modified Eagle's Medium [DMEM], Ascorbate-2-Phosphate, L-Proline,

Sodium Pyruvate, Insulin-transferrin-sodium selenite + Premix, and penicillin-streptomycin-fungizone [PSF]) or CM- supplemented with 10 ng/mL of IL-1 $\beta$  cytokine (human recombinant; Peptotech) for 2 weeks. These explants are fed every two to three days for a two-week period. MeHA was applied at the start of the study (t0), followed by 2 weeks of culture in IL-1 $\beta$ . After the conclusion of the culture, explants were subjected to the Hertzian creep indentation testing, as well as sulfated glycosaminoglycan (s-GAG) quantification, histological analysis, and immunofluorescence staining.

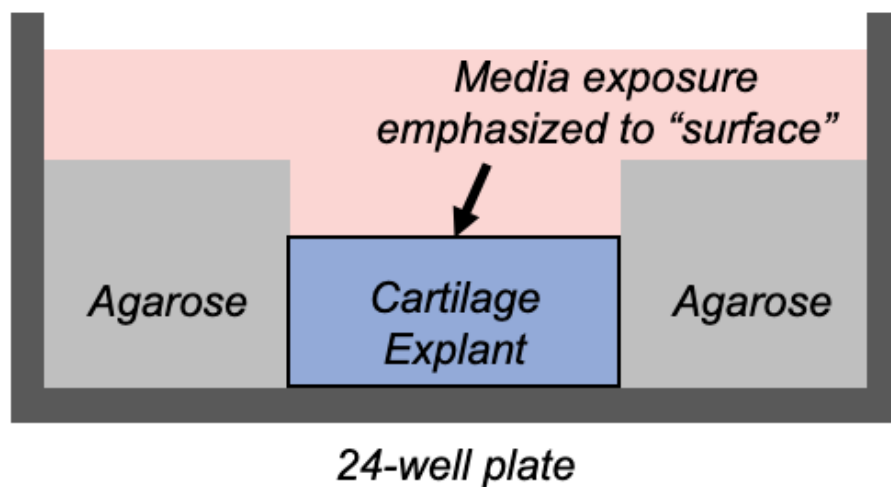


**Figure 12.** The MeHA hydrogel was integrated and crosslinked into the cartilage explants. The explants were then embedded into agarose wells to emphasize media exposure to the surface of the explant.

## 2.6 Mechanical Testing of Degenerative Culture

Creep experiments involve subjecting a material to a constant load and measuring the resulting deformation over time. In the case of cartilage, the creep behavior indicates its viscoelastic properties, which can be influenced by factors such as disease and mechanical damage. As articular cartilage is a complex tissue consisting of cells, extracellular matrix, and fluid, when it is subjected to compressive loads, the fluid is forced out of the tissue, causing a volume reduction and pressure increase. Over time, the degenerative environment of OA causes the tissue to undergo additional deformation in the extracellular matrix. In this case of damaged or diseased cartilage, the creep behavior may be altered.<sup>29,30</sup>

Cartilage explants were subjected to sequential Hertzian Indentation creep tests following biomaterial application and a 2-week degradation. Indentation creep testing is a time-dependent deformation under constant stress technique.<sup>29</sup> We specifically use the Hertzian Biphasic Theory (HBT) constant k method. This method is designed to fit a single creep curve to the HBT using constant permeability. Creep testing inputs on the Biomomentum Mach-1 include spherical probe radius ( $r=2\text{mm}$ ), tissue thickness, time (15 minutes), deformation, normal force (0.25N), and an initial guess. The method is fit with a Hertzian biphasic creep model<sup>29</sup> to output the compressive modulus ( $E_y^-$ ), tensile modulus ( $E_y^+$ ), permeability (k), and coefficient of determination ( $R^2$ ).

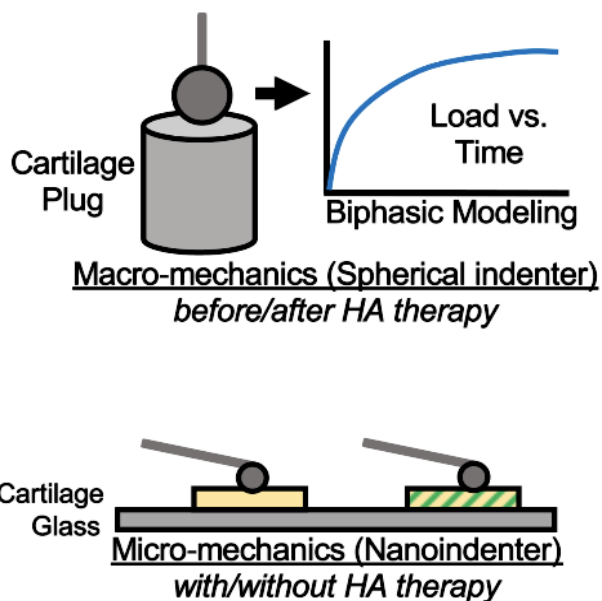


**Figure 13.** Hertzian indentation can be applied to cartilage explants to measure their mechanical properties. The sequential Hertzian indentation creep test involves performing multiple indentations at the same location on the cartilage and measuring its creep behavior, which is its tendency to deform under constant load over time. This measurement can provide insights into the mechanical properties of cartilage, which are essential for understanding its function and developing treatments for OA patients.<sup>27</sup>

Another output of the creep testing is permeability, an essential characteristic of cartilage that enables it to effectively perform its functions. Cartilage is an avascular tissue, therefore, relies on permeability for the diffusion of nutrients and waste products through its extracellular matrix to maintain its health and function. Permeability also plays a role in the lubrication of joints. The synovial fluid in the joint contains nutrients and lubricants that are transported through the cartilage matrix to reach the joint space, where it helps to reduce friction and wear on the joint surfaces. A low permeability is preferred as it allows fluid retention, which gives cartilage its shock absorbing properties.

## 2.7 DMMB Assay

Sulfated GAG (s-GAG) is a key signifier of degradation and is a product of proteoglycan and ECM breakdown. To determine s-GAG content of cultured explants, a dimethylmethylene blue (DMMB) assay was performed of culture media at days 3, 5, 7, 10, 12, and 14 of culture. The media was plated in duplicate in a 96-well assay plate (5uL), followed by addition of 200uL of 1,9-dimethylmethylene blue (8mg DMMB, 2.5mL ethanol, 1g sodium formate, 1mL formic acid, and 496.5mL deionized water). Absorbance values at 525nm were quantified relative to a standard curve of chondroitin sulfate (Sigma C-4384). s-GAG content was normalized as mass per dry weight of tissue, and also cumulatively added by time point to quantify cumulative release.

## 2.8 Safranin-O Fast Green Staining

Safranin-O has an affinity for sulfated proteoglycans within the extracellular cartilage matrix and stains red. Fast Green stains cartilage collagen fibers green, providing contrast and allowing for differentiation between the collagen-rich and proteoglycan-rich areas. Together, Safranin-O and Fast Green staining provide a practical way to visualize and analyze the structure and composition of cartilage tissue under a microscope. This is particularly useful in investigating cartilage development and degeneration.

Solutions of 0.05% w/v Fast green, 0.1% w/v Safranin O, and 1% v/v acetic acid were used. After mechanical testing, cartilage explants were cut in half vertically, fixed in formalin, and embedded in optical cutting temperature (OCT) compound. Explants were sectioned at 20µm and rinsed twice with DI H<sub>2</sub>O. The sections were then sequentially submerged for 5 minutes in Fast Green (0.05% w/v), 20 seconds in acetic acid (1% v/v), and 5 minutes in

Safranin O (0.1% w/v), followed by 2 tap water rinses, dehydration (95%, 100%, 2X each), clearing with Xylene, and mounting (Permount) and coverslipping for imaging.

## 2.9 Statistical analysis

Explants from at least 2 donors were included for each analysis to account for donor variability. All data was subject to outlier (ROUT method) and normality (Shapiro-Wilk) testing. Parametric, normal datasets were analyzed with a one-way analysis of variance (ANOVA) with post-hoc Tukey's testing. Nonparametric or non-normal datasets were analyzed with a Kruskal-Wallis test with post-hoc Dunn's Multiple Comparison Test. All data are shown as dot plots for transparency, and  $p < 0.05$  was chosen as a threshold for statistical significance.

### 3. Results

#### Aim 1: Methacrylation of Hyaluronic Acid and Gel Mechanics

##### 3.1 NMR of MeHA Polymers with Interpretations

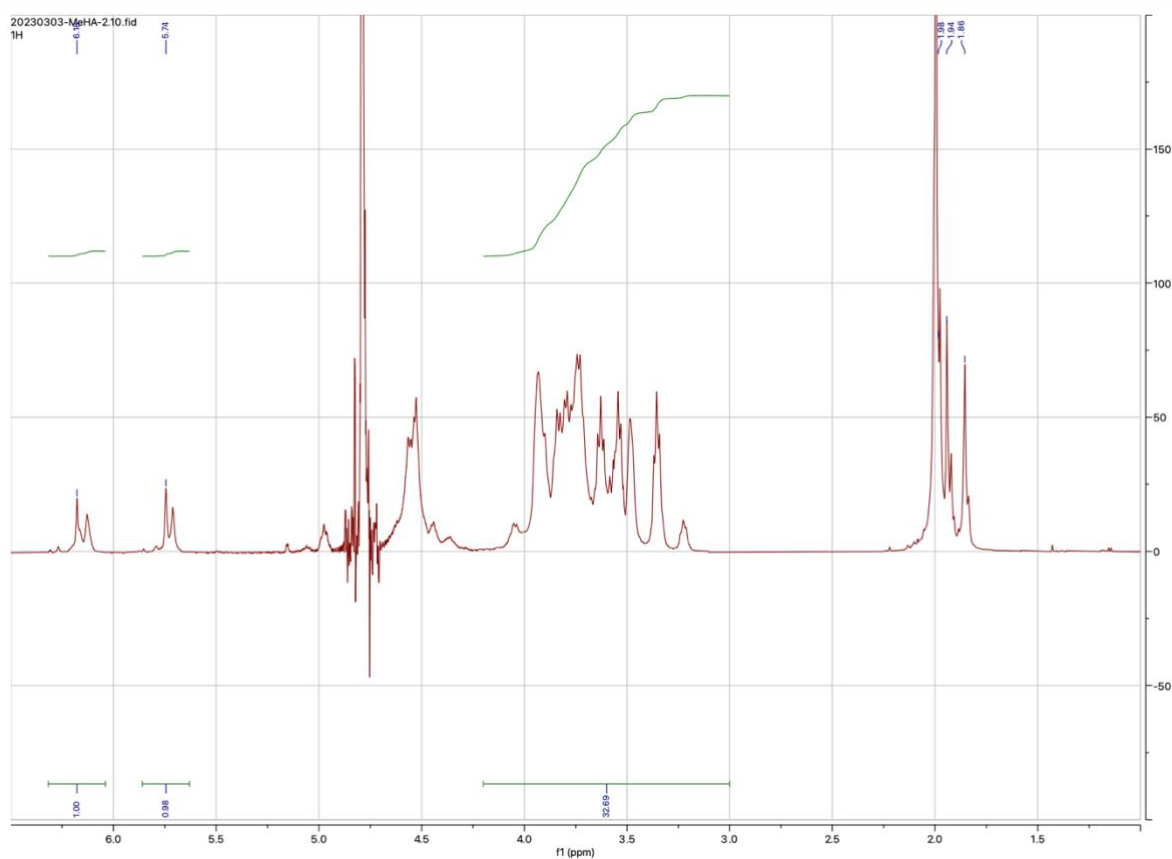


**Figure 14.** This NMR displays the 20 kDa MeHA polymer. Integration of the  $\delta$  6.2 ppm = 1.00,  $\delta$  5.8 ppm = 0.98, and  $\delta$  3.0–4.2 ppm = 32.69. This calculation resulted in a 30.28% methacrylation of the HA polymer.

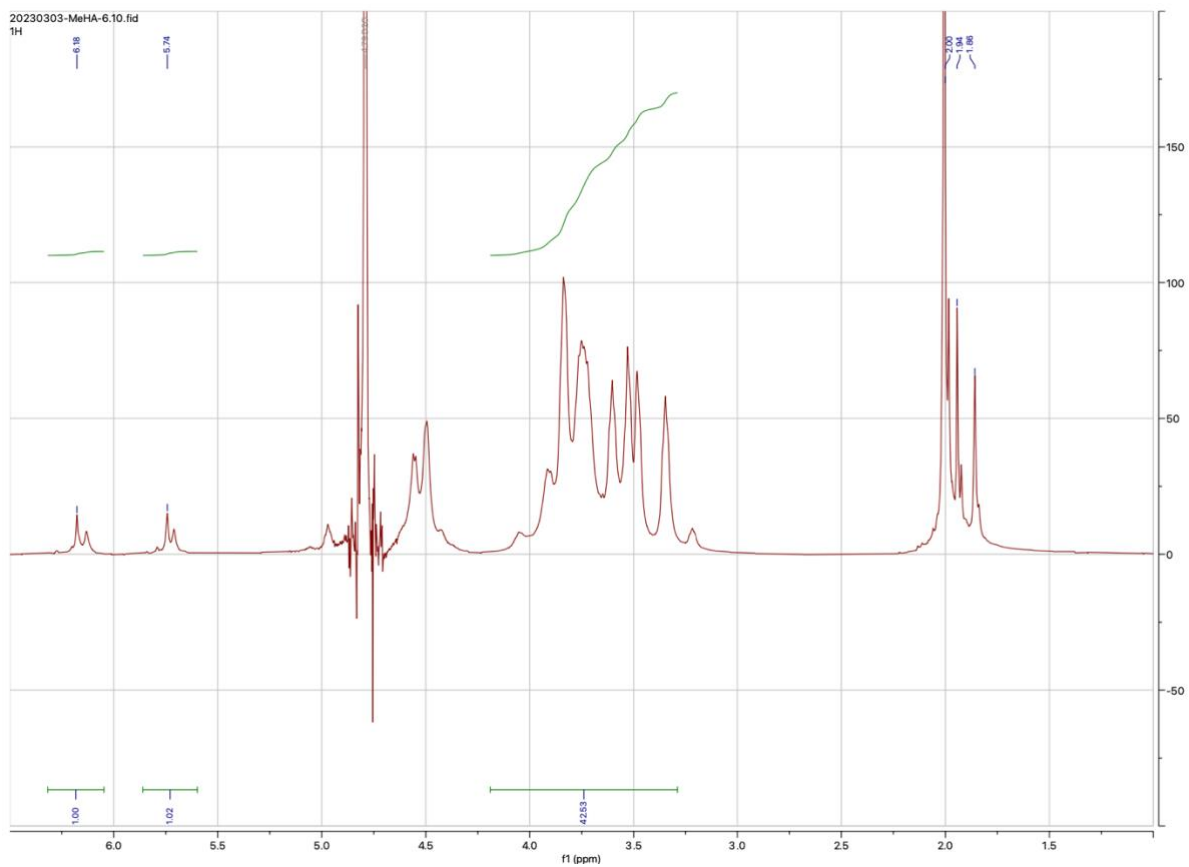


**Figure 15.** This NMR displays the 75 kDa MeHA polymer. Integration of the  $\delta$  6.2 ppm = 1.00,  $\delta$  5.8 ppm = 1.02, and  $\delta$  3.0–4.2 ppm = 42.53. This calculation resulted in a 35.5% methacrylation of the HA polymer.

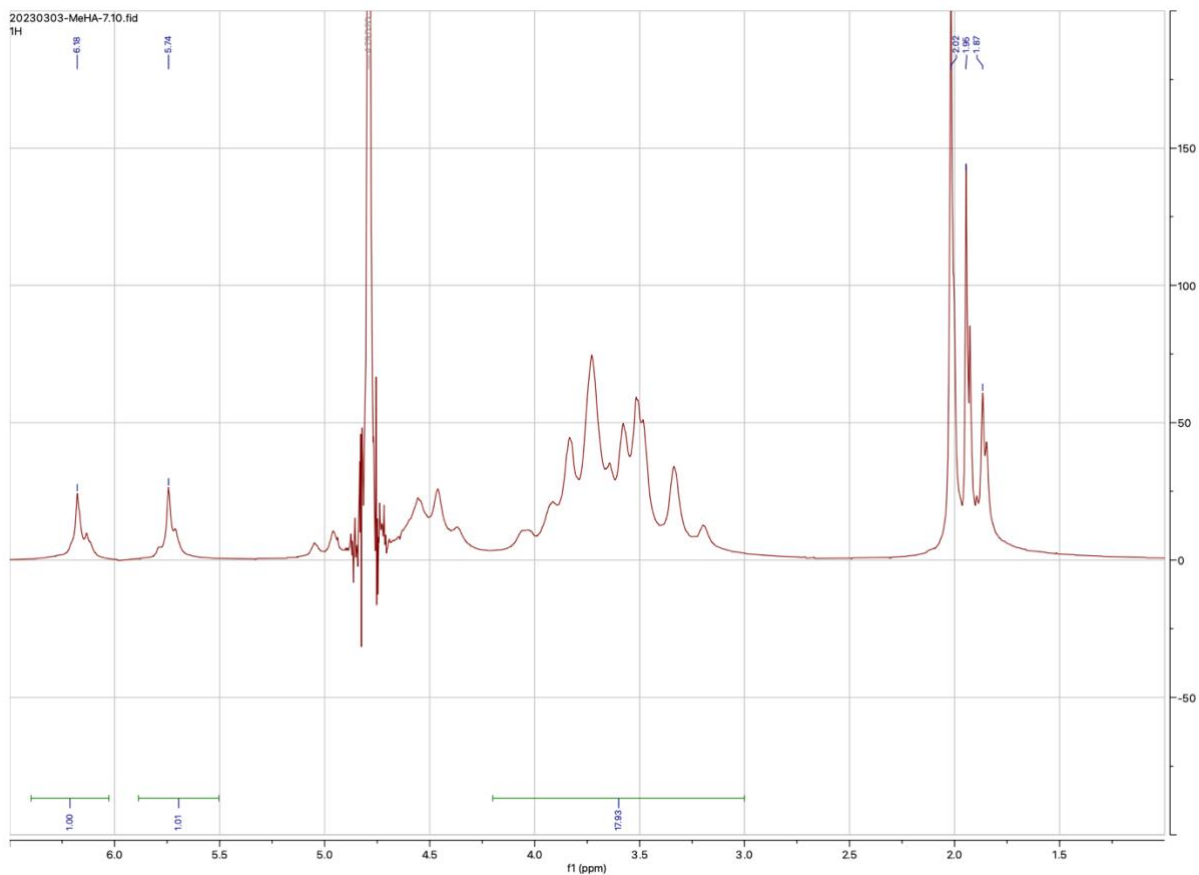


**Figure 16.** This NMR displays the 100 kDa MeHA polymer. Integration of the  $\delta$  6.2 ppm = 1.00,  $\delta$  5.8 ppm = 1.01, and  $\delta$  3.0–4.2 ppm = 17.98. This calculation resulted in a 55.9% methacrylation of the HA polymer.

Polymer	Percent Modification
<b>20</b>	30.28%
<b>75</b>	35.50%
<b>100</b>	55.90%

**Figure 17.** Following analysis of the NMR results in Mnova, we determined the percent methacrylate modification of each molecular weight polymer. The percent methacrylation is an important metric for determining the crosslinking ability of each MW MeHA polymer.

### 3.2 Gel Mechanics

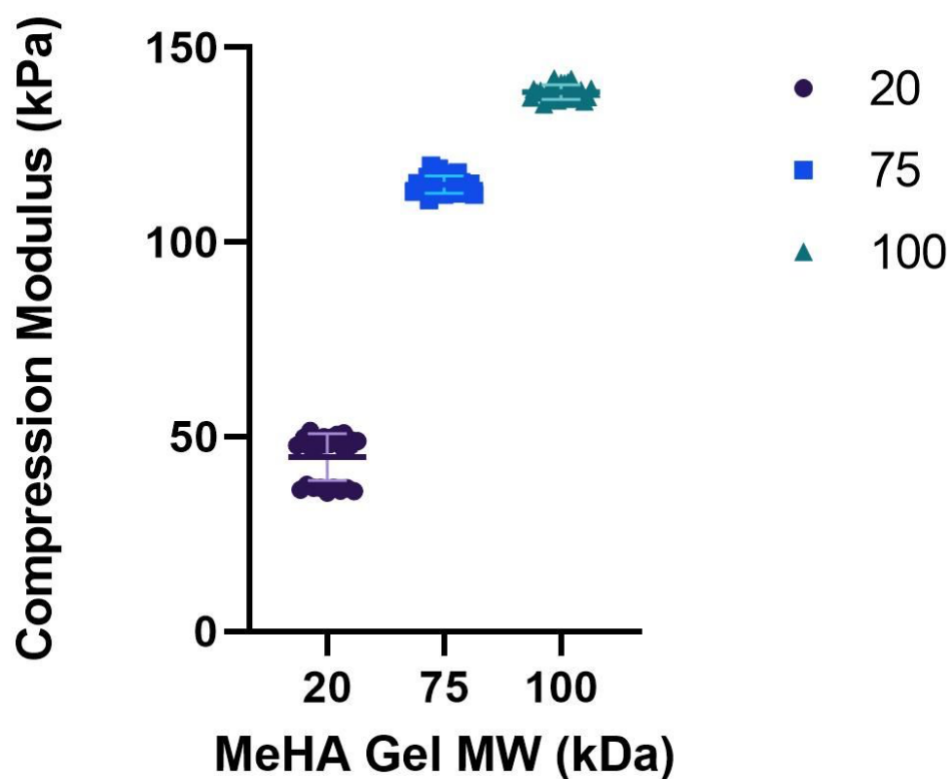


**Figure 18.** The compression modulus of three gel polymers, 20 kDa, 75 kDa, and 100 kDa is displayed above. All three gel polymers produced a statistically significant difference in compression modulus via one-way analysis of variance (ANOVA) with a \*\*\*\* P-value<0.0001 level of significance.

The compression modulus of each molecular weight condition differed to a significance level of p-value<0.0001. This serves as confirmation that each molecular weight hydrogel condition produces a significant difference regarding mechanical properties alone.

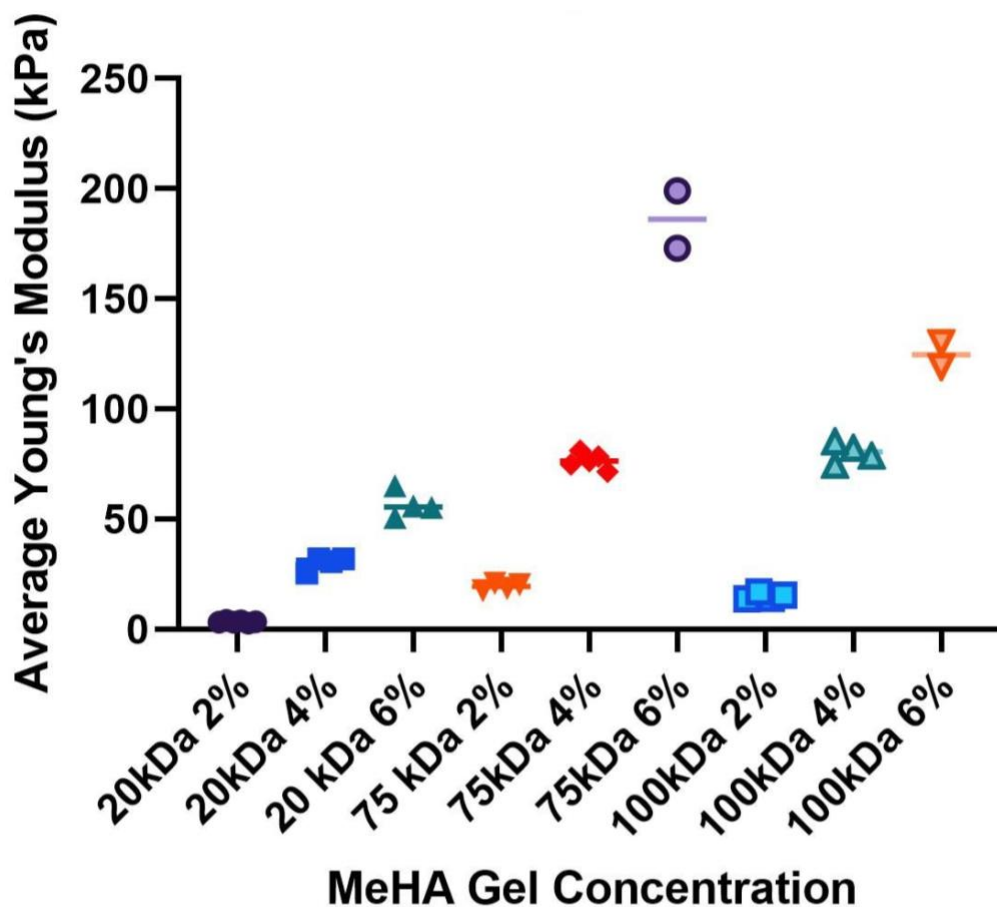


**Figure 19.** The compression modulus of three gel polymers, 20 kDa, 75 kDa, and 100 kDa is displayed at varying concentrations is depicted above.

The higher concentration gels exhibit a higher compressive modulus. This is expected as a higher concentration of polymer will allow for more crosslinking and a higher stiffness. We decided to perform our live explant degenerative culture with the 4% MeHA solution as the compressive modulus at this concentration shows the most clear positive correlation with polymer MW.

## Aim 2: MeHA Hydrogel Diffusion

### 3.3 Tissue Penetration of Degenerated Cartilage Images of Diffusion

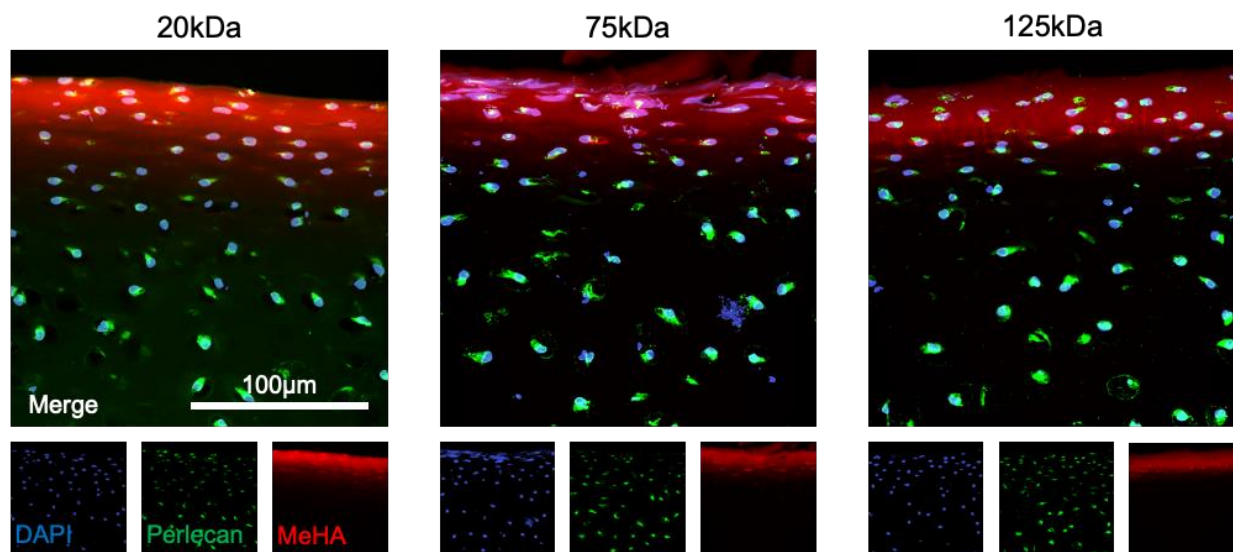


**Figure 20.** Above displays the images of the diffusion cartilage explants under TRITC filter overlaid with an image of the same explant viewed under a DAPI filter. The polymer material can be seen in red while the nuclei are blue.

Variation in the diffusion of the MeHA polymer can be observed in the above images.

The 20 kDa polymer appears to diffuse the most, followed by the 75 kDa polymer, and the 100 kDa polymer diffuses the least amount into the cartilage explants. This can be seen by the relative brightness of the methacrylated rhodamine, red region, which images the amount of polymer successfully diffused. This result aligned with our hypothesis of the 20kDa polymer diffusing the most.

### Aim 3: Application of MeHA to Living Explants

#### 3.4 Living Cartilage Explant Mechanics

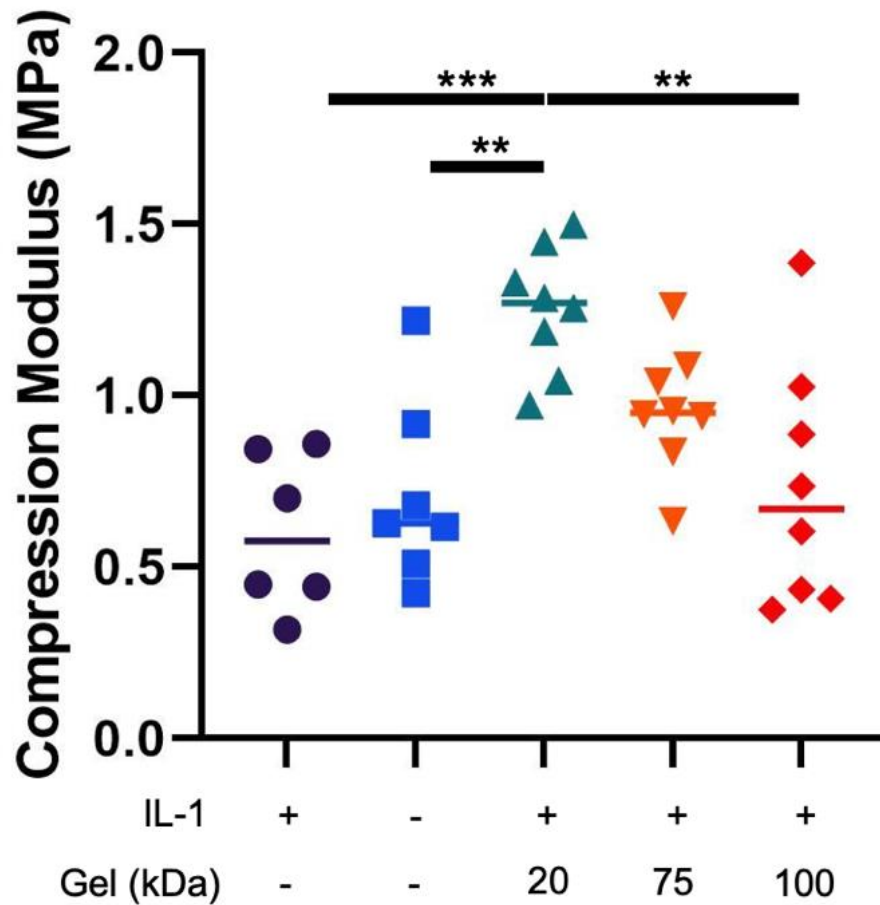


**Figure 21.** The compression modulus of the degenerative cultured cartilage explants is displayed above. The 20 kDa polymer produced a statistically significant difference with the IL-1, control, and 100 kDa polymer. \*\*\* P-value<0.001 and \*\* P-value<0.01

The 20 kDa polymer shows the greatest mechanical reinforcement and is statistically different than the control IL-1 condition.

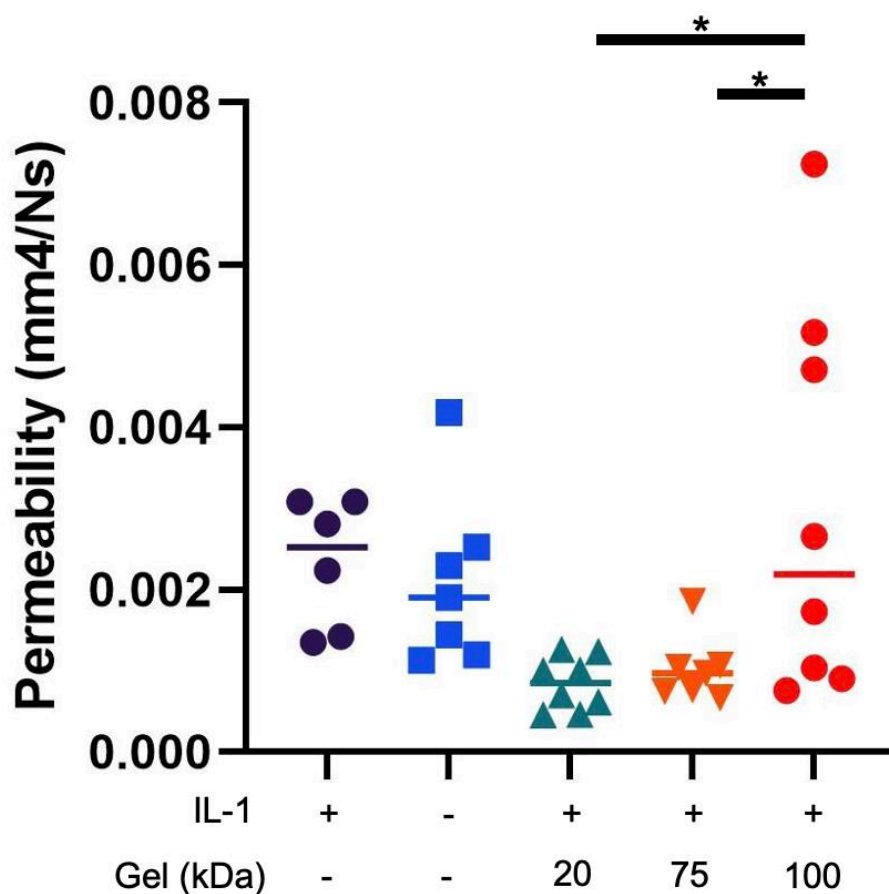


**Figure 22.** The permeability (k) of the degenerative cultured cartilage explants is displayed above. The 100 kDa polymer produced a statistically significant difference with the 20 kDa polymer and the 75 kDa polymer. \* P-value<0.05.

A low permeability is preferred as it allows fluid retention, which gives cartilage its shock absorbing properties. An increase in cartilage permeability is expected in a degrading environment.<sup>31</sup> It appears there is a non-favorable increase in permeability with the 100 kDa hydrogel and a maintained low permeability for the 20kDa and 75kDa conditions. However, there is no significant difference between the hydrogel conditions and the control or IL-1 conditions.

## 3.5 Proteoglycan Loss

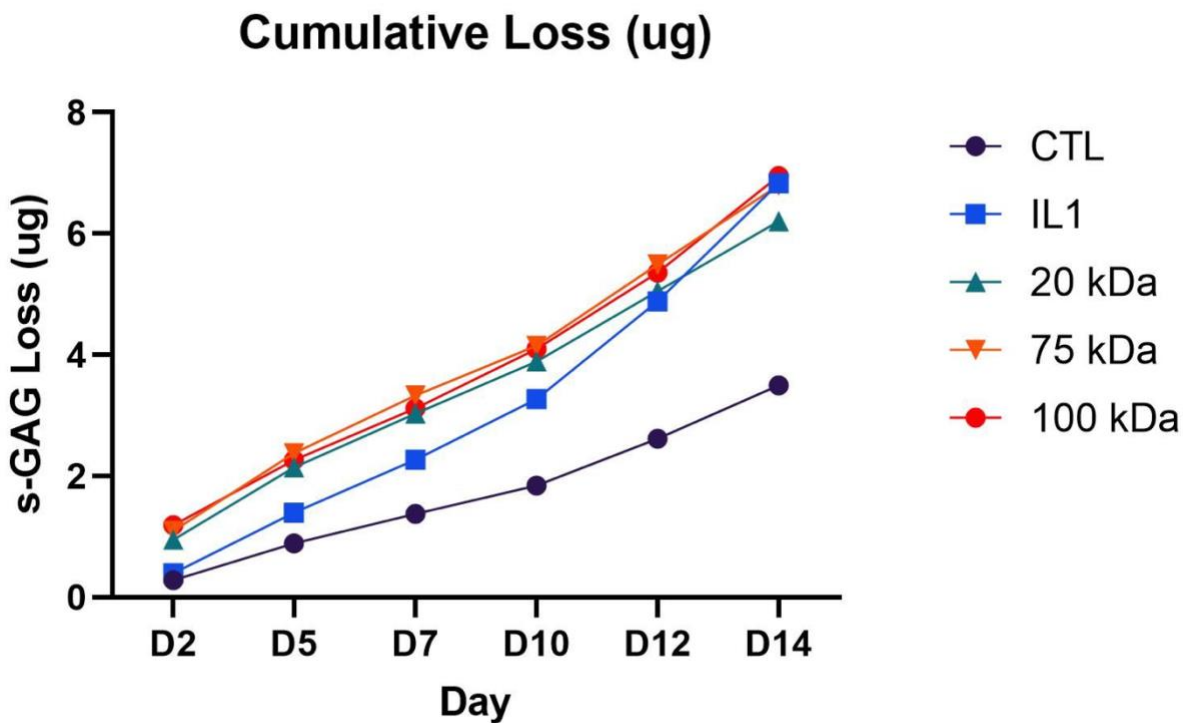


**Figure 23.** The GAG loss of the cartilage explants throughout the two-week degradation is depicted by day. GAG loss in articular cartilage refers to the depletion of glycosaminoglycans (GAGs), long chains of carbohydrates that are essential components of cartilage tissue. GAGs, such as chondroitin sulfate and keratan sulfate, are essential for articular cartilage's structure, function, and integrity, which is the smooth tissue that lines the ends of bones in joints.

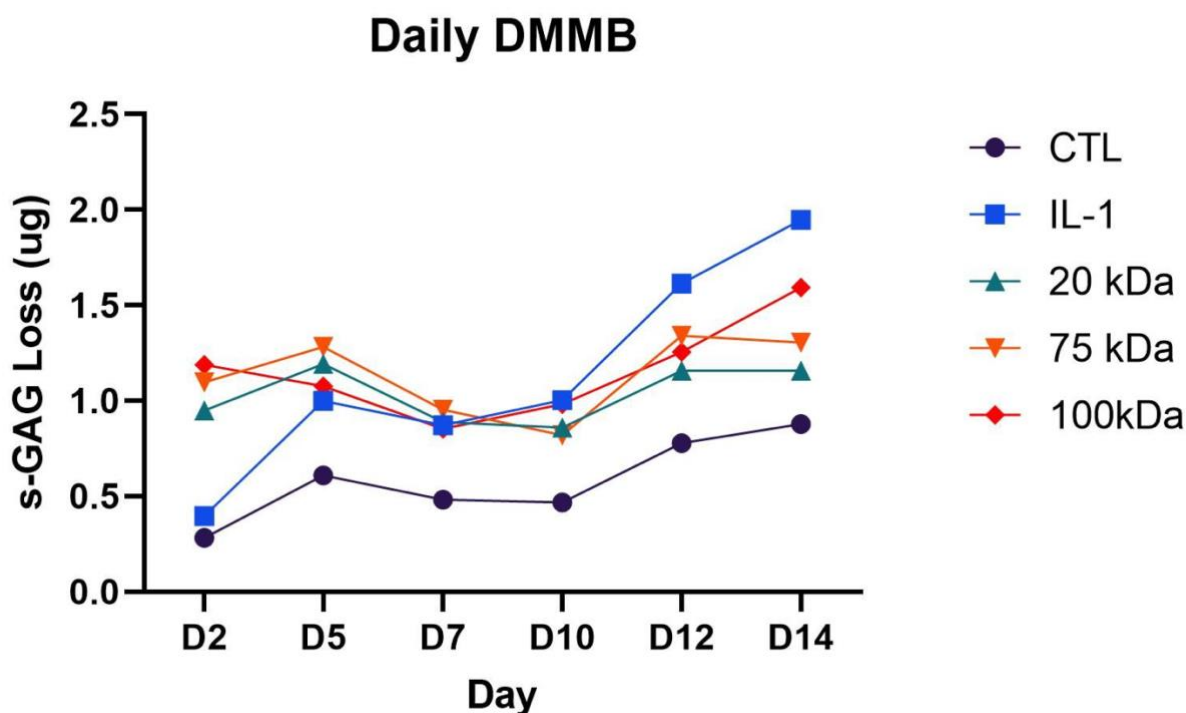


**Figure 24.** The daily GAG loss of the cartilage explants throughout the two-week degradation is depicted.

GAG studies did not appear to show any substantial reduction in cumulative proteoglycan loss. However, on day 14 of the daily DMMB, a relative difference in GAG loss can be seen, with 20kDa being more protective than 75kDa and 100kDa. The differences in GAG loss on day 14 are interesting as they follow the same trend in relative protective effects as the results from mechanical testing. The 20kDa being the most protective and the 100kDa being the least. Additionally, all MeHA hydrogel conditions appear to have a protective effect over IL-1 alone.

### 3.6 Imaging

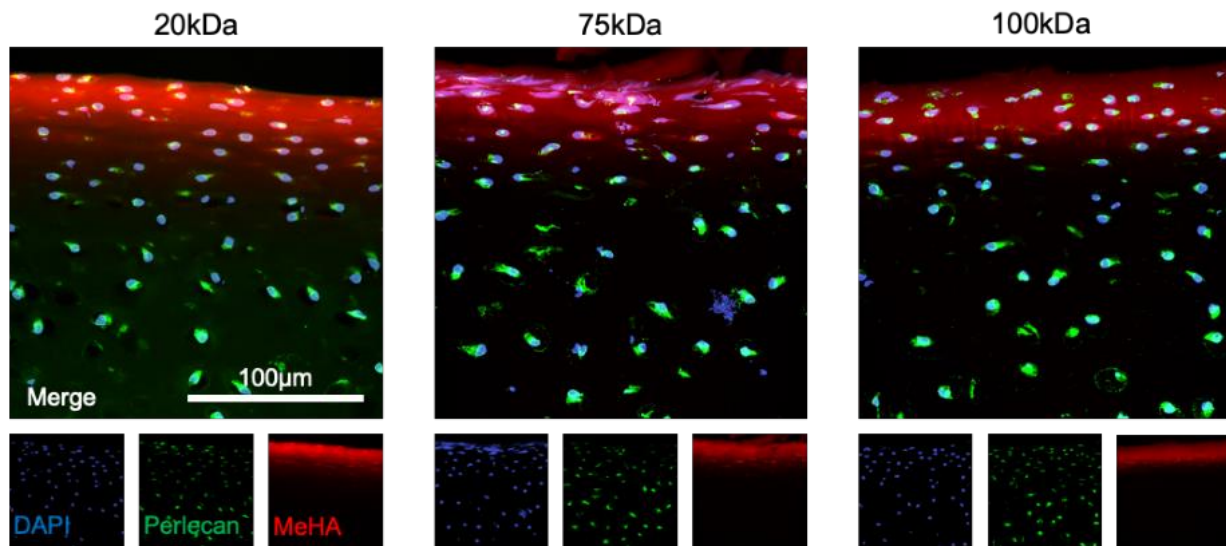


**Figure 25.** The imaging above depicts cartilage explants after the two-week degenerative culture. Qualitatively the brightest illuminating surface integrating polymer is the 20kDa followed by the 75kDa and 100kDa polymers.

The red fluorescence depicts the relative density of MeHA integration amongst the three groups. Qualitatively, the 20kDa MeHA appears to have the highest MeHA integration. Also imaged is DAPI which fluoresces the nucleus of the chondrocyte blue and Perlecan which fluoresces the pericellular matrix green.

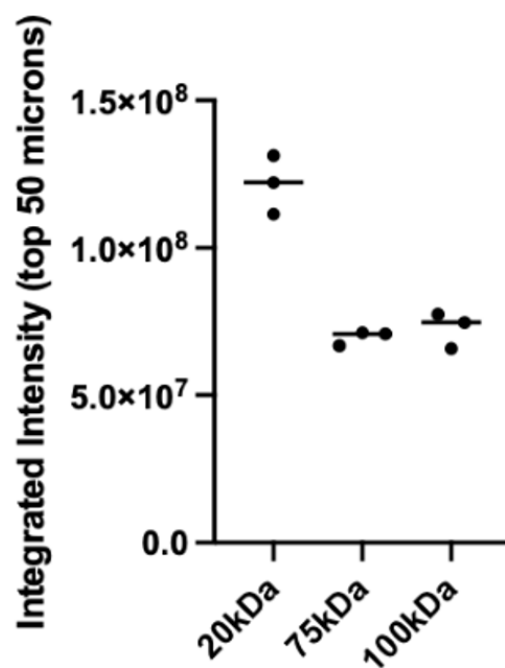


**Figure 26.** Quantitative analysis of the explant images from the two-week degenerative culture shows the greatest integrated surface intensity at the 20kDa explant. The 75kDa and 100kDa explants are very similar regarding integrated surface intensity.

## 4. Discussion

HA is of specific interest due to the biocompatibility of the polymer and its ability to provide structure for cell viability and proliferation at the articular cartilage level. This investigation studies the application of MeHA to the superficial zone of cartilage. This has a practical application to a focal defect scenario with little surface degeneration. Such a scenario refers to a situation where there is a localized area of damage or injury to a particular tissue, but the surrounding tissue is relatively healthy and intact. This could occur in the context of a traumatic injury to a joint, such as a knee. There may be a localized area of cartilage damage, the focal defect, where the cartilage has been torn or worn away. However, if the injury is caught early and treated appropriately, the surrounding cartilage and other joint structures may remain relatively healthy, with minor surface degeneration. The focus is on treating the localized area of damage or injury while also working to prevent further damage or deterioration of the surrounding tissue.

Throughout the experiment, differences in MeHA polymer MW were confirmed observationally. While synthesizing the hydrogel solution, the 100kDa polymer dissolved in PBS resulted in a more viscous solution than the 75 kDa and 20 kDa polymers. This viscosity difference was also observed between the 75 kDa and 20 kDa solutions, indicating an expected correlation between viscosity and molecular weight. Therefore, the difference in viscosity served as an observational confirmation of the differences in molecular weight among the solutions. Differences in MW were also confirmed statistically in gel mechanical testing. The gel

mechanical testing of the three different MW MeHA hydrogels produced a significant difference in hydrogel stiffness between all groups.

Nonsterile diffusion studies resulted in the 20kDa polymer being most diffuse. The diffusion of macromolecules through cartilage tends to be affected by the cartilage's local composition and structure, which varies with depth from the cartilage surface.<sup>32</sup> Our diffusion studies in the superficial zone showed a correlation between smaller MW MeHA polymer and a greater polymer surface integration density. This is expected from the literature as smaller macromolecules tend to show a greater diffusion in the superficial zone and 75kDa and 100kDa macromolecules tend to show a greater diffusion in the middle and deep zones.<sup>32</sup>

In the degenerative culture, the cumulative DMMB assay did not yield promising results in MeHA reducing proteoglycan loss in a degenerative environment. However, the daily DMMB study showed an interesting trend on the final day of the degenerative culture, day 14. The 20kDa MeHA polymer condition appeared to have the most protective effect followed by the 75kDa and 100kDa MeHA conditions compared to the IL-1 alone condition. This protective trend against proteoglycan loss on day 14 could point towards the prolonged fortification that MeHA provides for the cartilage (Figure 27).

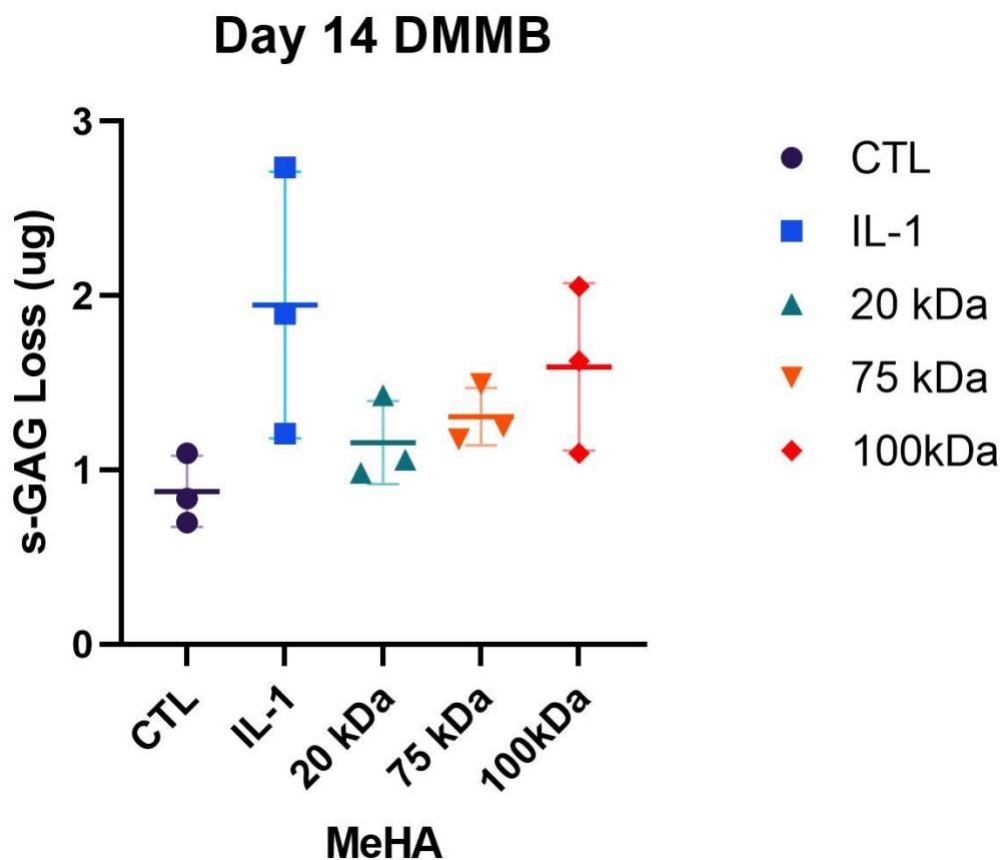


**Figure 27.** The DMMB assay at the final day of the degenerative culture shows an interesting trend in proteoglycan loss. This trend points towards possible long-term fortification of MeHA and the benefits the 20kDa polymer has over the other polymers.

It is important to note the hydrogel is a topical superficial zone application with integration into the cartilage surface. However, the agarose gel surrounding the cartilage explant plug does not protect against the IL-1 media. Therefore, proteoglycan loss can be occurring at any surface, not only where the hydrogel was applied.

The mechanical testing from the degenerative culture exhibited overall promising reinforcement under the 20 kDa MeHA polymer condition concerning the compressive modulus. The compressive modulus of cartilage is an important measure of its mechanical properties, as it reflects the tissue's ability to withstand compressive loads. In this experiment, we seek to

maintain the compressive modulus of the control. In our mechanical studies of the cartilage explants, it is important to note our control differs from the literature value of around 1 MPa. In this case of matching our experimental values with a control of 1 MPa, the 20 kDa polymer has a very promising protective effect. This is particularly surprising as this polymer has the lowest amount of methacrylation via NMR analysis but resulted in the most significant reinforcement. Additionally, this mechanical trend matches the same relative protective effects as the daily DMMB assay in the final day, day 14. Both results produced a similar trend of the 20kDa MeHA polymer being most protective followed the 75kDa polymer and the 100kDa polymer.

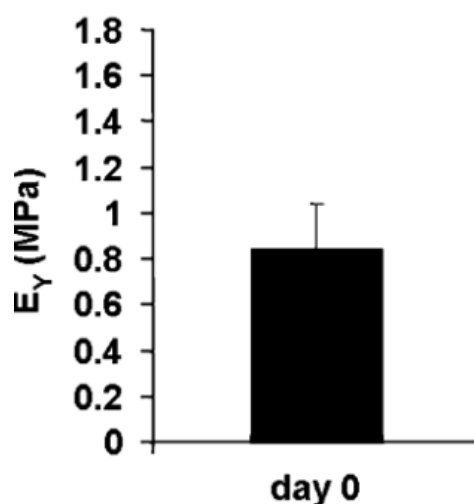


**Figure 28.** The image above portrays the average baseline from literature for juvenile bovine explant control compressive modulus.<sup>33</sup>

Previous studies have pointed towards higher molecular weight HA polymers being more effective in reducing the coefficient of friction (COF) of articular cartilage.<sup>34</sup> However, in focal defect scenarios where the COF is not yet an issue, preliminary treatment with low molecular weight MeHA could be more beneficial for delaying the progression of OA.

To further understand and advance the integration of hydrogels into cartilage, future studies could explore the role of polymer charge. Both HA and articular cartilage carry negative charges. Articular cartilage has a high concentration of negatively charged sulfate and carboxylate groups within the GAGs of the proteoglycan. The proteoglycan also contains negatively charged amino acids within its protein core. This negative charge promotes water accumulation within the cartilage matrix, contributing to its mechanical shock-absorbing and cushioning properties. Researchers could utilize this negative charge by designing a positively charged polymer to increase the attraction of the polymer to the cartilage and enhance hydrogel integration.

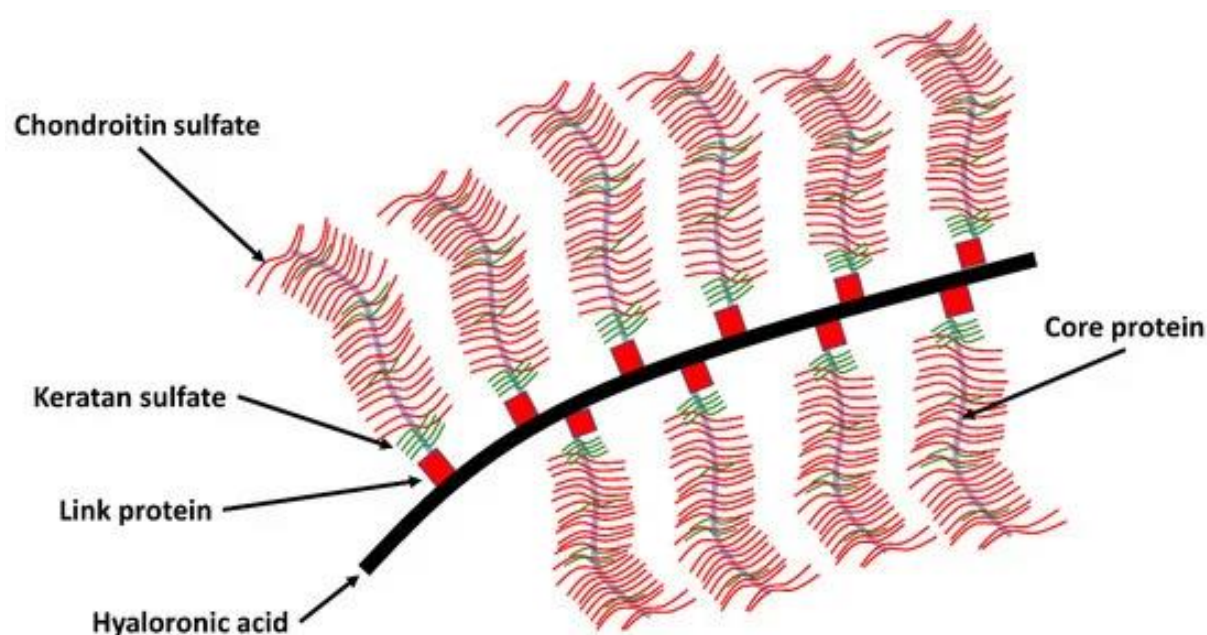


**Figure 28.** This image depicts the collagen and proteoglycan networks interreacting. Glycosaminoglycans such as keratan sulfate and chondroitin sulfate are attached to aggrecan.<sup>41</sup>

Differing the MW of MeHA hydrogels at different stages of degeneration could provide more information on the mechanism of MeHA hydrogel fortification of articular cartilage. The

20kDa could be best for the focal defect scenario. However, 75kDa or 100kDa MeHA might show more integration and fortification to degenerated articular cartilage.

## **5. Conclusion**

The results of the diffusion studies suggest a positive correlation between a smaller MW MeHA polymer and a higher integration density into the superficial zone. Additionally, the protective effects of the smaller MW MeHA polymer are further corroborated by the DMMB results on the final day of the degradative culture, indicating a superior ability to reduce proteoglycan loss compared to larger MW MeHA polymers. Furthermore, the compressive modulus of the smaller MW MeHA polymer maintains a desirable balance of stiffness and low permeability in the cartilage, supporting its mechanical efficacy.

## 6. Supplementary Information

### Abbreviation List:

OA = Osteoarthritis

NF-kB = Nuclear factor kappa B

HA = Hyaluronic Acid

IL = Interleukin

MeHA = Methacrylated hyaluronic acid

kDa = kilodalton

w/v = weight per volume

MWCO = molecular-weight cutoff

NMR = nuclear magnetic resonance

LAP = Lithium phenyl-2,4,6-trimethylbenzoylphosphinate

mW = milli Watts

PBS = phosphate-buffered saline

UV = ultraviolet

DMEM = Dulbecco's Modified Eagle's Medium

FBS = Fetal bovine serum

PSF = penicillin-streptomycin-fungizone

GAG = glycosaminoglycan

s-GAG = sulfated glycosaminoglycan

DMMB = dimethylmethylene blue

OCT = optimal cutting temperature

BSA = bovine serum albumin

DAPI = 4',6-diamidino-2-phenylindole

MMP = matrix metalloproteinase

ROUT = regression and outlier

ANOVA = analysis of variance

ECM = extracellular matrix

COF = coefficient of friction

## 7. References

1. Anatomy of the Knee | Arthritis Foundation. <https://www.arthritis.org/health-wellness/about-arthritis/where-it-hurts/anatomy-of-the-knee>.
2. OpenStaxCollege. Synovial Joints. (2013).
3. Sophia Fox, A. J., Bedi, A. & Rodeo, S. A. The Basic Science of Articular Cartilage. *Sports Health* **1**, 461–468 (2009).
4. Robinson, W. H. *et al.* Low-grade inflammation as a key mediator of the pathogenesis of osteoarthritis. *Nat. Rev. Rheumatol.* **12**, 580–592 (2016).
5. Liu, Y. *et al.* Exercise-induced piezoelectric stimulation for cartilage regeneration in rabbits. *Sci. Transl. Med.* **14**, eabi7282 (2022).
6. Osteoarthritis (OA) | Arthritis | CDC. <https://www.cdc.gov/arthritis/basics/osteoarthritis.htm> (2020).
7. CDC. Arthritis. *Centers for Disease Control and Prevention* <https://www.cdc.gov/chronicdisease/resources/publications/factsheets/arthritis.htm> (2021).
8. Bitton, R. The economic burden of osteoarthritis. *Am. J. Manag. Care* **15**, S230-5 (2009).
9. Arthritis Help for Veterans. <https://www.cdc.gov/arthritis/communications/features/arthritis-among-veterans.html> (2022).
10. Cameron, K. L., Hsiao, M. S., Owens, B. D., Burks, R. & Svoboda, S. J. Incidence of physician-diagnosed osteoarthritis among active duty United States military service members. *Arthritis Rheum.* **63**, 2974–2982 (2011).
11. Li, G. *et al.* Subchondral bone in osteoarthritis: insight into risk factors and microstructural changes. *Arthritis Res. Ther.* **15**, 223 (2013).

12. Shi, S., Mercer, S., Eckert, G. J. & Trippel, S. B. Regulation of articular chondrocyte catabolic genes by growth factor interaction. *J. Cell. Biochem.* **120**, 11127–11139 (2019).
13. Mabey, T. & Honsawek, S. Cytokines as biochemical markers for knee osteoarthritis. *World J. Orthop.* **6**, 95–105 (2015).
14. Kevorkian, L. *et al.* Expression profiling of metalloproteinases and their inhibitors in cartilage. *Arthritis Rheum.* **50**, 131–141 (2004).
15. de Lange-Brokaar, B. J. E. *et al.* Characterization of synovial mast cells in knee osteoarthritis: association with clinical parameters. *Osteoarthritis Cartilage* **24**, 664–671 (2016).
16. Mohamed, A. M. An Overview of Bone Cells and their Regulating Factors of Differentiation. *Malays. J. Med. Sci. MJMS* **15**, 4–12 (2008).
17. Suri, S. & Walsh, D. A. Osteochondral alterations in osteoarthritis. *Bone* **51**, 204–211 (2012).
18. Li, N. *et al.* Synovial membrane mesenchymal stem cells: past life, current situation, and application in bone and joint diseases. *Stem Cell Res. Ther.* **11**, 381 (2020).
19. Loeser, R. F., Goldring, S. R., Scanzello, C. R. & Goldring, M. B. Osteoarthritis: A Disease of the Joint as an Organ. *Arthritis Rheum.* **64**, 1697–1707 (2012).
20. Molnar, V. *et al.* Cytokines and Chemokines Involved in Osteoarthritis Pathogenesis. *Int. J. Mol. Sci.* **22**, 9208 (2021).
21. Ingegnoli, F. *et al.* The Crucial Questions on Synovial Biopsy: When, Why, Who, What, Where, and How? *Front. Med.* **8**, 705382 (2021).

22. Solanki, K., Shanmugasundaram, S., Shetty, N. & Kim, S.-J. Articular cartilage repair & joint preservation: A review of the current status of biological approach. *J. Clin. Orthop. Trauma* **22**, 101602 (2021).
23. Falah, M., Nierenberg, G., Soudry, M., Hayden, M. & Volpin, G. Treatment of articular cartilage lesions of the knee. *Int. Orthop.* **34**, 621–630 (2010).
24. Patel, J. M. *et al.* Stabilization of Damaged Articular Cartilage with Hydrogel-Mediated Reinforcement and Sealing. *Adv. Healthc. Mater.* **10**, e2100315 (2021).
25. Hintze, V., Schnabelrauch, M. & Rother, S. Chemical Modification of Hyaluronan and Their Biomedical Applications. *Front. Chem.* **10**, 830671 (2022).
26. Wei, W. *et al.* Advanced hydrogels for the repair of cartilage defects and regeneration. *Bioact. Mater.* **6**, 998–1011 (2020).
27. Kowalski, M. A. *et al.* Cartilage-penetrating hyaluronic acid hydrogel preserves tissue content and reduces chondrocyte catabolism. 2022.05.17.492335 Preprint at <https://doi.org/10.1101/2022.05.17.492335> (2022).
28. Ma, W. & Suh, W. H. Cost-Effective Cosmetic-Grade Hyaluronan Hydrogels for ReNcell VM Human Neural Stem Cell Culture. *Biomolecules* **9**, 515 (2019).
29. Moore, A. C., DeLuca, J. F., Elliott, D. M. & Burris, D. L. Quantifying Cartilage Contact Modulus, Tension Modulus, and Permeability With Hertzian Biphasic Creep. *J. Tribol.* **138**, (2016).
30. Gong, H., Men, Y., Yang, X., Li, X. & Zhang, C. Experimental Study on Creep Characteristics of Microdefect Articular Cartilages in the Damaged Early Stage. *J. Healthc. Eng.* **2019**, 8526436 (2019).

31. Cooper, B. G., Lawson, T. B., Snyder, B. D. & Grinstaff, M. W. Reinforcement of articular cartilage with a tissue-interpenetrating polymer network reduces friction and modulates interstitial fluid load support. *Osteoarthritis Cartilage* **25**, 1143–1149 (2017).
32. Leddy, H. A. & Guilak, F. Site-specific molecular diffusion in articular cartilage measured using fluorescence recovery after photobleaching. *Ann. Biomed. Eng.* **31**, 753–760 (2003).
33. Bian, L. *et al.* Mechanical and biochemical characterization of cartilage explants in serum-free culture. *J. Biomech.* **41**, 1153–1159 (2008).
34. Rebenda, D., Ranuša, M., Čípek, P., Toropitsyn, E. & Vrbka, M. In Situ Observation of Hyaluronan Molecular Weight Effectiveness within Articular Cartilage Lubrication. *Lubricants* **11**, 12 (2023).
35. Zhang, J. *et al.* Harnessing hyaluronic acid for the treatment of osteoarthritis: A bibliometric analysis. *Front. Bioeng. Biotechnol.* **10**, 961459 (2022).
36. Kim, Y. S. & Guilak, F. Engineering Hyaluronic Acid for the Development of New Treatment Strategies for Osteoarthritis. *Int. J. Mol. Sci.* **23**, 8662 (2022).
37. Tsanaktsidou, E., Kammona, O. & Kiparissides, C. On the synthesis and characterization of biofunctional hyaluronic acid based injectable hydrogels for the repair of cartilage lesions. *Eur. Polym. J.* **114**, 47–56 (2019).
38. Koh, R. H., Jin, Y., Kim, J. & Hwang, N. S. Inflammation-Modulating Hydrogels for Osteoarthritis Cartilage Tissue Engineering. *Cells* **9**, 419 (2020).
39. Fahy, N., Farrell, E., Ritter, T., Ryan, A. E. & Murphy, J. M. Immune modulation to improve tissue engineering outcomes for cartilage repair in the osteoarthritic joint. *Tissue Eng. Part B Rev.* **21**, 55–66 (2015).

40. Lagneau, N. *et al.* Harnessing cell-material interactions to control stem cell secretion for osteoarthritis treatment. *Biomaterials* **296**, 122091 (2023).
41. Eschweiler, J. *et al.* The Biomechanics of Cartilage—An Overview. *Life* **11**, 302 (2021).